

Spectroscopy of ^{230}Th in the (p,t) reactionA. I. Levon,^{1,*} G. Graw,² Y. Eisermann,² R. Hertenberger,² J. Jolie,³ N. Yu. Shirikova,⁴ A. E. Stuchbery,⁵
A. V. Sushkov,⁴ P. G. Thirolf,² H.-F. Wirth,² and N. V. Zamfir⁶¹*Institute for Nuclear Research, Academy of Science, Kiev, Ukraine*²*Fakultät für Physik, Ludwig-Maximilians-Universität München, Garching, Germany*³*Institut für Kernphysik, Universität zu Köln, Köln, Germany*⁴*Joint Institute for Nuclear Research, Dubna, Russia*⁵*Department of Nuclear Physics, Australian National University, Canberra, Australia*⁶*H. Hulubei National Institute of Physics and Nuclear Engineering, Bucharest, Romania*

(Received 25 July 2008; published 30 January 2009)

The excitation spectra in the deformed nucleus ^{230}Th were studied by means of the (p,t) reaction, using the Q3D spectrograph facility at the Munich Tandem accelerator. The angular distributions of tritons are measured for about 200 excitations seen in the triton spectra up to 3.3 MeV. Firm 0^+ assignments are made for 16 excited states by comparison of experimental angular distributions with the calculated ones using the CHUCK code. Additional assignments are possible, with assignments for four states relatively firm and another four tentative. Assignments up to spin 6^+ are made for other states. Sequences of the states are selected that can be treated as rotational bands and as multiplets of excitations. Experimental data are compared with interacting boson model (IBM) and quasiparticle-phonon model (QPM) calculations.

DOI: [10.1103/PhysRevC.79.014318](https://doi.org/10.1103/PhysRevC.79.014318)

PACS number(s): 21.10.-k, 21.60.-n, 25.40.Hs, 27.90.+b

I. INTRODUCTION

A full microscopic description of low-lying excitations in deformed nuclei has eluded theoretical studies to date. Along with the interplay of collective and single-particle excitations, which takes place in deformed rare-earth nuclei, additional problems arise in the actinide region because of the reflection asymmetry [1]. Evidently, the nature of the first excited 0^+ states in the actinide nuclei is different from that in the rare-earth region, where they are due to the quadrupole vibration [2]. Octupole degrees of freedom have to be important in the actinides. One has then to expect a complicated picture at higher excitations: Residual interactions could mix the one-phonon and multiphonon vibrations of quadrupole and octupole character with each other and with quasiparticle excitations. Detailed experimental information on the properties of such excitations is needed for comparison with theory. On the experimental side, the (p,t) reaction is very useful. On the theoretical side, a microscopic approach such as the quasiparticle-phonon model (QPM) is necessary to account for the number of states detected and to make detailed predictions on their properties.

Our previous paper [3] concentrated on the excited 0^+ states in the actinide nuclei ^{228}Th , ^{230}Th , and ^{232}U studied in the (p,t) reaction. This interest in the 0^+ excitations in the deformed actinide nuclei was stimulated by the observation of multiple $L = 0$ transfers in the (p,t) reaction leading to the excited states in the odd nucleus ^{229}Pa [4] as well as to the excited states in the medium heavy even nuclei ^{146}Nd [5], ^{146}Sm [6], and $^{132,134}\text{Ba}$ [7]. After comprehensive information on 0^+ excitations was obtained in the actinide nuclei [3], systematic studies of the same type were made on many nuclei

between ^{152}Gd and ^{192}Hg [8] and revealed a large number of excited 0^+ states, whose nature is not yet understood. The (p,t) reaction, however, gives much more extensive information on specific excitations in these nuclei, which was not analyzed previously [3]. An attempt to obtain such information was made for ^{168}Er after using a high-resolution experimental study with the (p,t) reaction [9]. In this paper we present the results of a careful and detailed analysis of the experimental data from the high-precision, high-resolution study of the $^{232}\text{Th}(p,t)^{230}\text{Th}$ reaction carried out to get deeper insight into excitations in ^{230}Th including the nature of the 0^+ excitations.

Experimentally accessible thorium nuclei span a wide and interesting range of isotopes: from the semimagic ^{216}Th to quadrupole-deformed ^{234}Th . An especially interesting region is that around $A = 228$, where the even isotopes ^{226}Th , ^{228}Th , and ^{230}Th are considered to be octupole deformed, octupole soft, and vibrational-like, respectively [10]. Two of them are accessible for study by the (p,t) reaction. Besides 0^+ excitations, whose number is increased in comparison with the preliminary analysis in publication [3], the spins for many other states are also assigned. The results concerning 0^+ , 2^+ , and 4^+ excitations are mainly discussed. The 6^+ and negative-parity states are excited weakly in the (p,t) reaction; therefore information on these states is only fragmentary. The results of a similar analysis for ^{228}Th in comparison with ^{229}Pa as well as for ^{232}U will be presented in forthcoming papers [11].

In Sec. II A of this paper the details of the experimental techniques and the experimental results are given. After a description of the distorted-wave Born approximation (DWBA) analysis a preliminary treatment of the nature of some excitations is presented. In Sec. III the interpretation of 0^+ excitations is discussed. The experimental data obtained in this study are compared with the results of calculations in the microscopic approach of the QPM. The validity of the

*levon@kinr.kiev.ua

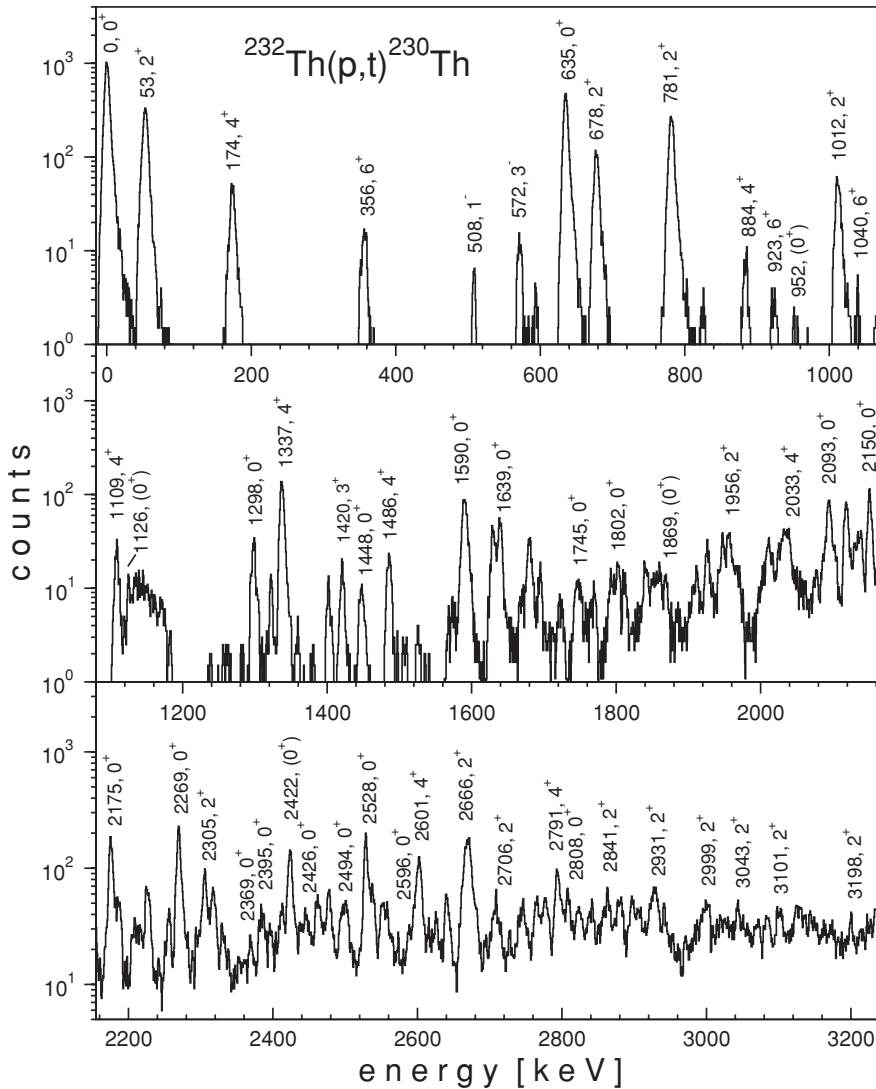


FIG. 1. Triton energy spectrum from the $^{232}\text{Th}(p,t)^{230}\text{Th}$ reaction ($E_p = 25$ MeV) on a logarithmic scale for a detection angle of 7.5° . Some strong lines are labeled with the corresponding level energies in keV and by the spins assigned from the DWBA fit.

phenomenological approach of the interacting boson model (IBM) is also tested to account for at least the main features of the positive-parity excitations in ^{230}Th , in addition to 0^+ states tested in Ref. [3].

II. EXPERIMENT, ANALYSIS, AND EXPERIMENTAL DATA

A. Details of the experiment

A target of $100 \mu\text{g}/\text{cm}^2$ ^{232}Th evaporated on a $22 \mu\text{g}/\text{cm}^2$ thick carbon backing was bombarded with 25-MeV protons of an intensity of $1\text{--}2 \mu\text{A}$ from the Tandem accelerator of the Maier-Leibnitz-Labor of the Ludwig-Maximilians-Universität and Technische Universität München. The isotopic purity of the target was about 99%. The tritons were analyzed with the Q3D magnetic spectrograph and then detected in a focal plane detector. The focal plane detector is a multiwire proportional chamber with readout of a cathode foil structure for position determination and dE/E particle identification [12,13]. The acceptance of the spectrograph was 11 msr, except for the most forward angle of 5° with an acceptance of 6 msr.

The resulting triton spectra have a resolution of 4–7 keV (FWHM) and are background free for all angles but 5° , for which background from light contaminations in the region of 1100–1150 keV complicated the analysis for some levels. The angular distributions of the cross sections were obtained from the triton spectra at 10 laboratory angles from 5° to 45° .

A triton energy spectrum measured at a detection angle of 7.5° , shown in Fig. 1, demonstrates the domination of 0^+ excitations having large cross sections at this angle. The analysis of the triton spectra was performed with the program GASPAN [14]. Measurements were carried out with two magnetic settings: one for excitations up to 1.6 MeV and another for the energy region from 1.5 to 3.3 MeV. For the calibration of the energy scale the triton spectra from the reactions $^{184}\text{W}(p,t)^{182}\text{W}$, $^{186}\text{W}(p,t)^{184}\text{W}$, and $^{234}\text{U}(p,t)^{232}\text{U}$ were measured at the same magnetic settings. Some known levels in ^{230}Th were included in the calibration, leading to small corrections from 0 to 0.5 keV for excitations between 1.5 and 3.3 MeV. In the course of our measurements we found that the Q values for the (p,t) reactions on the ^{232}Th , ^{230}Th , and ^{234}U targets or on the ^{186}W and ^{184}W targets are in disagreement with the ones calculated from the Atomic Mass Evaluation

TABLE I. Q values for the (p,t) reactions as determined from a comparison of the experimental triton spectra and as derived from the AME 2003 compilation [15].

Reaction	Ref.: $^{232}\text{Th}(p,t)$ (keV)	Ref.: $^{184}\text{W}(p,t)$ (keV)	AME 2003 [15] (keV)
$^{232}\text{Th}(p,t)$	-3076.5(27)	-3064.2(20)	-3076.5(27)
$^{230}\text{Th}(p,t)$	-3568.5(30)	-3556.6(20)	-3569.0(28)
$^{234}\text{U}(p,t)$	-4125.2(30)	-4113.0(20)	-4124.2(29)
$^{186}\text{W}(p,t)$	-4478.1(30)	-4460.5(20)	-4463.0(19)
$^{184}\text{W}(p,t)$	-5133.0(30)	-5120.6(12)	-5120.6(12)

(AME) [15] depending upon which Q value is used as the reference value. They are given in Table I. The notation ‘‘Ref.’’ (the reference value) in this table means that the Q value for this nucleus as determined from the data in the AME was taken as a starting point in the calculations for other nuclei. If the Q value for the $^{232}\text{Th}(p,t)$ reaction as derived from Ref. [15] is taken as the reference value, then the Q values for $^{230}\text{Th}(p,t)$ and $^{234}\text{U}(p,t)$ reactions also agree with those calculated from the AME table [15]. However, the Q values for the $^{186}\text{W}(p,t)$ and $^{184}\text{W}(p,t)$ reactions differ considerably from the calculated one and vice versa, if the Q value for the $^{184}\text{W}(p,t)$ reaction is taken as the reference value. The reason for this discrepancy is not clear from these data.

About 200 levels have been identified in the spectra for all 10 angles and these are listed in Table II. The energies and spins of the levels as derived from this study are compared to known energies and spins from the published data [16–18]. They are given in the first four columns. The ratios of cross sections at angles 5° and 26° to that at angle 16° , given in the next two columns, help to highlight the 0^+ excitations (large values). The column σ_{integ} gives the cross section integrated in the region from 5° to 45° and the column $\sigma_{\text{exp}}/\sigma_{\text{calc}}$ gives the

ratio of the integrated cross sections, from experimental values and calculations in the DWBA (see Sec. II B). The last column lists the notational schemes used in the DWBA calculations: sw,jj means one-step direct transfer of the $(j)^2$ neutrons in the (p,t) reaction; notation for the multiway transfers used in the DWBA calculations are displayed in Fig. 6 (see Sec. II B).

To get an indication of the possible 0^+ excitations at higher energies, the triton spectra were measured for the angles of 12.5° and 26.0° and in the energy range from 2.8 to 4.5 MeV. A precise calibration of this region of excitations is not possible with the spectra measured for the tungsten and uranium targets or any other targets. Therefore the calibration makes use of that employed for the energy region 1550–3300 keV with a linear shift of the energy and channel number determined from the position of the known levels observed in both energy regions. The measured spectra are compared in Fig. 2. The ratio of the line intensities at 2808 keV in two spectra can serve as a reference for the 0^+ state assignments. Peaks that may correspond to the excitation of 0^+ states are marked by dashed lines. Unfortunately, close values of the excitation ratios are valid also for 6^+ and 3^+ excitations, as shown by the states at 3052 and 3072 keV. Nevertheless, at least 10 candidates for 0^+ excitations are revealed in the region from 3 to 4 MeV. Measurements at an angle of 5° could confirm or reject these assumptions.

B. DWBA analysis

The spins of the excited states in the final nucleus ^{230}Th were assigned via an analysis of the angular distributions of tritons from the (p,t) reaction. In a previous publication [3] the angular distributions for 0^+ excitations were demonstrated to have a steeply rising cross section at very small reaction angles and a sharp minimum at a detection angle of about 14° .

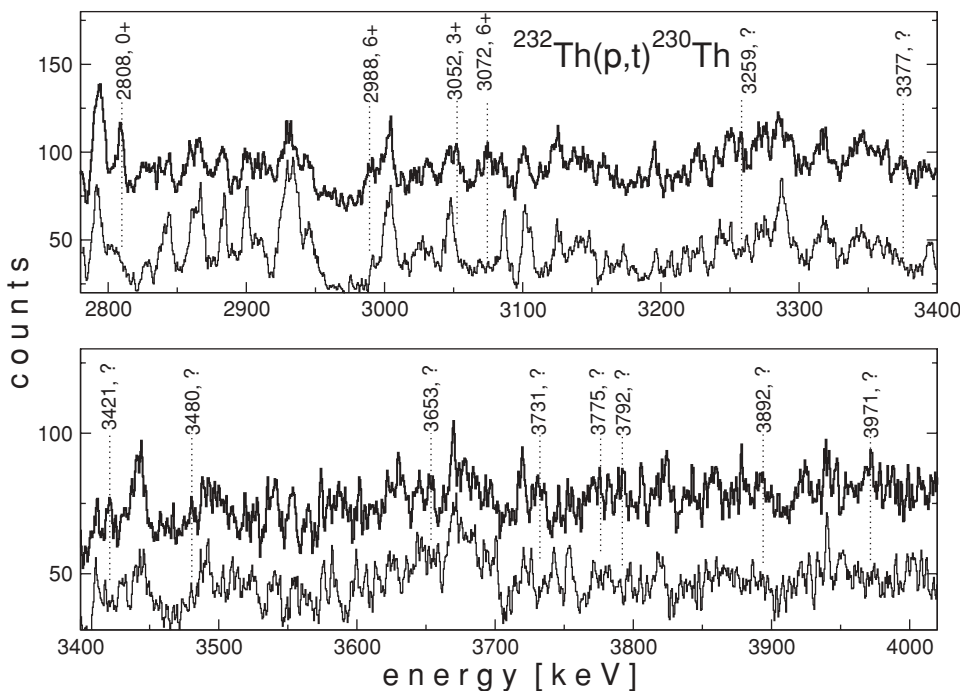


FIG. 2. Comparison of the spectra for the $^{232}\text{Th}(p,t)^{230}\text{Th}$ reaction ($E_p = 25$ MeV) for detection angles of 12.5° (thin line) and 26° (thick line) for the high-energy range. The lines corresponding to possible 0^+ excitations are labeled by their energies.

TABLE II. Energies of levels in ^{230}Th , the level spin assignments from the CHUCK analysis, the (p,t) cross sections integrated over the measured values, and the reference to the schemes used in the DWBA calculations (see text for more detailed explanations).

Level energy (keV)		I^π		Cross-section ratios		σ_{integ} (μb)	Ratio $\sigma_{\text{exp}}/\sigma_{\text{calc}}$	Way of fitting
This work	Refs. [16–18]	Refs. [16–18]	This work	($5^\circ/16^\circ$)	($26^\circ/16^\circ$)			
0.1 2	0.0	0 ⁺	0 ⁺	8.02	5.51	195.68	10.7	sw.gg
53.2 2	53.20 2	2 ⁺	2 ⁺	1.57	0.27	52.53	11.0	m1a
174.0 2	174.10 3	4 ⁺	4 ⁺	0.87	0.50	9.94	2.6	m1a
356.3 2	356.6 5	6 ⁺	6 ⁺	0.40	0.75	7.39	2.8	m2d
508.0 3	508.15 3	1 ⁻	1 ⁻	0.63	0.00	0.87	0.6	m2a
571.7 2	571.73 3	3 ⁻	3 ⁻	0.33	0.44	4.04	0.8	m3a
593.8 3	594.1 5	8 ⁺	8 ⁺	1.05	0.00	0.37	0.4	m2c
635.1 2	634.88 5	0 ⁺	0 ⁺	26.91	8.92	47.79	250	sw.ii
677.6 2	677.54 5	2 ⁺	2 ⁺	0.85	0.55	25.13	3.5	m1a
686.0 10	686.7	5 ⁻				<0.2		
775.2 4	775.5 3	4 ⁺	4 ⁺	0.30	0.53	7.15	1.3	m1a
781.4 2	781.35 3	2 ⁺	2 ⁺	0.62	0.46	69.07	6.2	sw.gg
825.6 3	825.66 5	3 ⁺	3 ⁺	0.14	0.79	1.10	2.5	m2a
852.7 4	851.88 3	7 ⁻				0.42		
884.2 4	883.9 2	4 ⁺	4 ⁺	0.51	1.27	4.09	0.8	m1a
923.3 5	923.0 2	6 ⁺	6 ⁺	1.66	0.96	0.50	0.2	m2d
952.6 5	951.88 5	1 ⁻	1 ⁻	1.17	1.76	0.71	0.03	m1a ^a
			or (0 ⁺)				0.6	sw.ij ^a
	955.1 2	5 ⁺						
972.1 5	971.72 5	2 ⁻	2 ⁻	0.22	0.69	0.37	5.0	m2a
1011.6 5	1009.58 5	2 ⁺	2 ⁺	0.54	0.34	14.34	2.1	sw.gg
	1012.51 5	3 ⁻	3 ⁻				6.0	sw.gg
1040.0 7	1039.6 2	6 ⁺	6 ⁺	0.80	1.07	0.94	0.5	m2a
1052.0 7	1052.31 5	3 ⁺	3 ⁺	0.00	3.33	0.34	0.8	m2a
1065.9 8			4 ⁻	0.99	0.69	0.30	0.45	m3b
1079.4 8	1079.21 3	2 ⁻	2 ⁻	0.00	0.00	0.09	0.1	m3b
1108.7 5	1107.5 3	4 ⁺	4 ⁺	1.20	0.87	5.38	1.2	m2a
	1109.0 1	5 ⁻						
	1117.5 3	8 ⁺						
1125.6 5			(1 ⁻)	4.54	1.06	2.10	0.1	m1a ^a
			or (0 ⁺)				1.5	sw.jj ^a
	1127.76 5	3 ⁻						
	1134.4 2	7 ⁺						
1148.0 9						<0.2		
	1176.1 3	5 ⁺						
1184.8 9						<0.2		
	1196.8	(4 ⁻)						
1241.2 9	1243.3 3	8 ⁺				<0.2		
1256.0 9	1255.5 3	6 ⁺				<0.2		
1259.2 6			(3 ⁻)	0.97	0.34	0.34	0.3	sw.gg
1283.6 6			(5 ⁻)	1.08	0.00	0.23	0.07	m3b
1297.8 6	1297.1 1	0 ⁺	0 ⁺	4.37	2.53	4.15	1.8	sw.ig
1322.3 5			(3 ⁻)	1.23	0.54	1.77	1.5	sw.gg
1337.2 5			4 ⁺	1.37	1.14	24.42	3.2	sw.gg
	1349.3 4	7 ⁺						
1359.5 7			(2 ⁺)	0.00	0.41	0.48	0.05	sw.gg
1376.6 7	1375.3 1	1, 2 ⁺	1 ⁺ , 5 ⁻	0.00	0.00	0.24	0.2/0.1	m3b
1401.5 5	1400.9 1	2 ⁺	2 ⁺	0.49	0.38	3.18	0.3	sw.gg
1420.4 5			(3 ⁺)	0.33	0.70	4.74	1.0	m2a
1440.4 8			(3 ⁺)			<0.2		
1447.9 5			0 ⁺	10.37	6.86	1.70	0.05	sw.gg
1485.6 5	1485.6 1		4 ⁺	1.44	0.93	4.59	0.6	sw.gg
1496.0 10						<0.2		
1507.4 5			4 ⁺	1.29	2.28	0.57	0.07	m2a
1524.8 5			2 ⁺	0.66	0.00	0.53	0.05	sw.gg

TABLE II. (Continued.)

Level energy (keV)		I^π		Cross-section ratios		σ_{integ} (μb)	Ratio $\sigma_{\text{exp}}/\sigma_{\text{calc}}$	Way of fitting
This work	Refs. [16–18]	Refs. [16–18]	This work	($5^\circ/16^\circ$)	($26^\circ/16^\circ$)			
1566.2 6			(1 ⁻)	1.80	0.29	0.31	0.15	m2b
1574.5 6	1573.5 2		(2 ⁻)	0.34	0.70	2.14	3.8	m2a
1584.7 6			(4 ⁻ , 5 ⁺)	1.77	1.90	2.64	42/36	m2a
1590.2 5	1589.8 2		0 ⁺	8.48	6.04	11.66	0.28	sw.gg
1594.7 8			(1 ⁻)	1.11	0.58	2.22	1.5	m3b
1601.2 11			(3 ⁻)	1.46	1.14	0.74	0.8	sw.gg
1612.1 10			(4 ⁻ , 5 ⁺)	1.26	2.25	0.36	8.3/1	m2a
1618.7 9			(4 ⁻ , 5 ⁺)	1.44	2.09	0.27	8.0/0.9	m2a
1630.1 7	1628 2		2 ⁺	1.43	0.45	4.49	0.6	m1a
1639.3 6	1638.5 2		(2, 0 ⁺)	5.68	4.64	8.32	0.2	sw.gg
1653.2 11			(6 ⁺)	0.96	1.75	0.88	0.004	m3a
1668.2 7			4 ⁺	1.54	1.85	1.91	0.3	sw.gg
1679.1 7			2 ⁺	1.72	0.36	3.36	0.45	m1a
1683.3 7			(4 ⁻)	0.19	1.95	2.20	34	m2a
1694.9 7	1695.7 1		(4 ⁺)	1.09	1.41	3.57	0.35	sw.gg
1708.8 8			2 ⁺	0.22	0.18	0.38	0.03	sw.gg
1723.5 7			(4 ⁺)	0.55	1.35	2.31	0.3	m1a
1745.3 8	1744.9 1		0 ⁺	2.80	2.59	1.18	0.10	sw.jg
1750.7 8			(3 ⁻)	1.76	0.64	0.99	0.8	sw.gg
1762.3 8			(4 ⁺)	0.73	0.43	0.89	0.2	m1a
1769.6 8	1770.7 1		(4 ⁺)	0.52	0.69	0.89	0.15	sw.gg
1774.1 9	1775.2 1		1, 2 ⁺			<0.2		
	1789.4 5		1 ⁽⁻⁾ , 2 ⁺					
1793.1 6			(5 ⁻)	1.19	1.19	2.43	3.5	sw.gg
1802.5 6			0 ⁺	8.04	5.38	2.38	0.05	sw.gg
	1810.7 1		1, 2 ⁺					
1812.0 8			4 ⁺	1.71	0.96	1.26	0.13	sw.gg
1824.9 7			(6 ⁺)	0.45	0.96	1.15	0.15	sw.gg
1840.0 8	1839.6 2		2 ⁺	1.74	0.70	2.37	0.25	m1a
1851.4 7	1849.6 1		(3 ⁻)	1.07	0.93	1.73	1.5	sw.gg
1859.3 7	1858.2 6		(3 ⁻)	1.41	1.05	1.74	1.6	sw.gg
1868.9 7			(0 ⁺)	1.99	1.60	1.73	0.03	sw.gg ^b
			+ (6 ⁺)				0.26	m2d ^b
1887.0 9			(2 ⁺)	0.84	0.68	0.76	0.06	sw.gg
	1902.7 1		1, 2 ⁺					
1910.0 9			(6 ⁺)	0.51	1.13	1.84	0.25	sw.gg
1914.7 9			(1 ⁻)	0.91	0.57	1.18	0.8	m2a
1926.0 7			4 ⁺	2.18	0.90	1.71	0.6	m2a
1931.1 8			(1 ⁻)	0.81	0.50	0.62	0.5	m2a
1939.8 11			(1 ⁻ , 1 ⁺)	0.36	0.68	0.98	0.6	m2a
1947.0 6			4 ⁺	1.18	0.89	3.81	0.4	m1a
	1949.8 1		1, 2 ⁺					
1956.4 6			2 ⁺	0.39	0.47	6.96	0.35	sw.gg
1967.1 7	1966.9 2		1, 2 ⁺	0.27	0.66	3.76	0.18	sw.gg
1972.0 9	1973.4 2		(1 ⁺ , 2 ⁺)	0.58	0.39	0.94	0.05	sw.gg
1985.4 8			(5 ⁻)	0.00	0.52	0.51	0.8	sw.gg
2001.6 8	2000.9 1		1, 2 ⁺	1.28	0.83	1.15	1.1	sw.gg
2010.3 6	2010.1 2		1, 2 ⁺	0.26	0.38	5.69	0.3	sw.gg
2017.3 7			(3 ⁻)	1.03	0.73	1.75	1.6	sw.gg
2025.6 6	2024.7 2		1 ⁺ , 2 ⁺	0.28	0.39	3.84	0.2	sw.gg
2032.8 7			4 ⁺	1.07	1.13	5.69	0.5	sw.gg
2039.1 7			4 ⁺	2.24	1.85	4.51	0.4	sw.gg
2048.7 7			(4 ⁺)	1.00	1.19	1.59	0.15	sw.gg
2060.9 12			(3 ⁻)	2.05	0.55	0.87	0.02	m3a
2073.2 8			(8 ⁺)	0.00	1.82	1.40	0.4	sw.gg
2074.9 8			(4 ⁺)	0.85	0.51	1.16	0.2	m1a

TABLE II. (*Continued.*)

Level energy (keV)		I^π		Cross-section ratios		σ_{integ} (μb)	Ratio $\sigma_{\text{exp}}/\sigma_{\text{calc}}$	Way of fitting
This work	Refs. [16–18]	Refs. [16–18]	This work	($5^\circ/16^\circ$)	($26^\circ/16^\circ$)			
2085.9 8			(4 ⁺)	1.75	1.26	1.60	0.15	sw.gg
2093.9 7			0 ⁺	4.44	2.17	6.93	13	sw.ii
2102.0 7			4 ⁺	2.30	1.10	1.26	0.15	sw.gg
2118.4 6			4 ⁺	2.32	1.14	7.70	0.90	sw.gg
2130.7 7	2122.8 1	1, 2 ⁺	2 ⁺	0.51	0.76	5.23	0.2	sw.gg
2137.9 7	2133.2 2		2 ⁺	0.51	0.50	4.87	0.2	sw.gg
2150.5 6			0 ⁺	10.53	3.87	6.57	25	sw.ii
2168.8 7	2151.8 2	1, 2 ⁺	(4 ⁺)	1.12	1.37	2.31	0.2	sw.gg
2175.1 6			0 ⁺	21.75	8.97	11.93	42	sw.ii
2181.7 7			(4 ⁺)	1.02	2.07	4.22	0.35	sw.gg
2187.1 6			2 ⁺	0.39	0.57	8.14	0.30	sw.gg
2194.8 8			(6 ⁺)			0.59	0.25	m2a
2205.4 10			2 ⁺	0.49	0.47	2.67	0.10	sw.gg
2207.8 8			(4 ⁺)	1.99	2.40	2.74	0.2	sw.gg
2216.0 7			(4 ⁺)	1.07	0.44	1.62	0.4	m2a
2226.0 6			2 ⁺	0.56	0.54	9.84	0.5	sw.gg
2241.0 7			2 ⁺	0.29	0.49	1.13	0.06	sw.gg
2249.9 7			(6 ⁺)	0.46	1.22	1.54	0.2	sw.gg
2255.3 7			4 ⁺	1.81	1.41	3.79	0.4	sw.gg
2268.9 6			0 ⁺	15.37	6.16	14.86	56	sw.ii
2276.0 8			(4 ⁺)	0.00	2.02	1.59	0.15	sw.gg
2282.1 10	2282.8 5	1, 2 ⁺	4 ⁺	3.08	1.78	2.20	0.25	sw.gg
2295.9 8	2298.6 3	1, 2 ⁺	2 ⁺	0.52	0.53	13.62	0.7	sw.gg
2305.4 7			(4 ⁺)	0.41	1.20	2.33	0.2	sw.gg
2311.2 8	2314.3 2	1, 2 ⁺	4 ⁺	2.75	1.27	4.95	0.5	sw.gg
2317.7 7			2 ⁺	0.37	0.34	2.65	0.1	sw.gg
2329.6 7			(5 ⁻)	0.90	0.87	1.28	2.0	sw.gg
2337.1 8			(6 ⁺)	2.12	2.20	0.60	1.6	m2a
2354.8 10	2368.9 2		(0 ⁺)	2.75	3.79	1.70	0.23	sw.jg
2368.5 7			(4 ⁺)	1.02	0.87	4.54	0.3	m2a
2383.8 8						1.32		
2388.4 10			0 ⁺	3.95	2.14	0.94	2.8	sw.ii
2395.2 7			(6 ⁺)	0.50	0.70	0.89	0.4	m2a
2402.0 8			2 ⁺	0.30	0.60	6.39	0.3	sw.gg
2411.6 7			(4 ⁺)	3.20	1.87	8.3	0.8	sw.gg ^b
2422.7 7			+ (0 ⁺)			5.2	7.5	sw.ii ^b
2426.4 9			(0 ⁺)	3.11	2.30	3.50	6.7	sw.ii
2436.6 9			2 ⁺	0.33	0.49	2.20	0.10	sw.gg
2442.5 8			2 ⁺	0.65	0.68	3.73	0.15	sw.gg
2449.2 2			(3 ⁻)	1.34	0.71	1.65	1.6	sw.gg
2461.0 7			2 ⁺	0.41	0.62	8.08	0.4	sw.gg
2467.2 7			2 ⁺ , 3 ⁻	0.49	0.79	3.55	0.15	sw.gg
2474.3 8			2 ⁺	0.15	0.50	5.20	0.25	sw.gg
2478.5 8			4 ⁺	2.20	1.00	5.00	0.5	sw.gg
2481.3 12			(6 ⁺)	0.03	0.16	1.21	0.5	m2a
2493.8 7			0 ⁺	5.62	3.92	3.40	1.4	sw.ig
2501.1 7			4 ⁺	1.43	1.41	4.70	0.6	sw.gg
2508.3 7				0.00	1.68	0.76		
2519.3 7			(6 ⁺)	0.00	1.13	1.43	0.5	m2a
2528.1 7			0 ⁺	11.96	6.76	12.36	5.6	sw.ig

TABLE II. (Continued.)

Level energy (keV)		I^π		Cross-section ratios		σ_{integ} (μb)	Ratio $\sigma_{\text{exp}}/\sigma_{\text{calc}}$	Way of fitting
This work	Refs. [16–18]	Refs. [16–18]	This work	($5^\circ/16^\circ$)	($26^\circ/16^\circ$)			
2536.9 7			4^+	1.36	1.43	6.07	0.6	sw.gg
2549.8 11			0^+	4.32	2.60	2.75	1.2	sw.ig
2556.2 8			(4^+)	0.85	1.10	4.05	0.75	m1a
2562.9 9			(4^+)	0.00	0.83	1.56	0.2	sw.gg
2573.2 7			(6^+)	0.00	1.18	1.33	0.5	m2a
2589.1 7			2^+	0.49	0.64	3.92	0.15	sw.gg
2596.4 8			(0^+)	31.20	10.35	2.50	5.1	sw.ii
2601.3 7			(4^+)	1.34	0.93	14.48	2.8	m2a
2616.0 7			2^+	0.55	0.61	2.76	0.4	sw.gg
2625.9 7			2^+	0.37	0.40	4.41	0.15	sw.gg
2640.0 8			4^+	1.83	1.55	7.41	0.7	sw.gg
2660.9 7			4^+	2.92	2.29	4.24	0.3	sw.gg
2666.4 7			(2^+)	0.34	0.58	26.48	1.5	sw.gg
2671.6 7			4^+	1.77	1.07	11.82	1.2	sw.gg
2679.2 8			2^+	0.39	0.30	3.77	0.15	sw.gg
2694.9 7			2^+	0.49	0.43	1.25	0.06	sw.gg
2706.5 7			2^+	0.79	0.53	6.14	0.2	sw.gg
2712.9 8			(6^+)	0.74	1.17	2.84	1.0	m2a
2726.6 7			2^+	1.02	0.87	2.28	0.1	sw.gg
2740.6 7			2^+	0.33	0.41	5.13	0.15	sw.gg
2746.2 7			4^+	3.35	1.84	2.77	0.3	sw.gg
2754.2 10			(6^+)	1.47	1.19	1.26	0.2	sw.gg
2764.9 7			2^+	0.66	0.70	8.03	0.3	sw.gg
2777.3 7			2^+	0.78	0.51	7.89	0.3	sw.gg
2791.5 7			4^+	1.77	1.09	11.49	1.2	sw.gg
2799.7 8			2^+	0.25	0.51	3.01	0.1	sw.gg
2808.1 7			0^+	7.72	3.30	4.86	8.5	sw.ii
2824.4 10			4^+	2.63	1.35	3.03	0.4	sw.gg
2834.0 10			2^+	0.18	0.69	2.58	0.2	sw.gg
2841.3 7			(2^+)	0.54	0.97	4.26	0.3	sw.gg
2855.9 7			2^+	0.51	0.82	4.04	0.3	sw.gg
2862.9 7			2^+	0.58	0.74	6.25	0.4	sw.gg
2870.6 10			(3^-)	1.50	0.93	1.26	1.2	sw.gg
2879.7 7			2^+	0.76	0.62	5.49	0.5	sw.gg
2886.1 10			(1^-)	1.71	0.49	0.99	0.8	m2a
2896.1 7			2^+	0.32	0.51	5.52	0.5	sw.gg
2906.4 8			(3^-)	0.75	1.07	3.42	2.6	sw.gg
2913.6 15			(4^+)	0.51	0.37	1.60	0.12	sw.gg
2923.7 9			2^+	0.51	0.85	5.87	0.4	sw.gg
2930.6 7			2^+	0.49	0.50	6.31	0.26	sw.gg
2940.6 7			2^+	0.37	0.53	3.84	0.3	sw.gg
2950.5 8			(6^+)	0.20	1.41	0.99	0.5	m2a
2987.9 10			(6^+)	0.49	0.96	3.75	0.6	sw.gg
2999.0 7			2^+	0.46	0.71	7.66	0.6	sw.gg
3009.9 8			2^+	0.34	0.67	2.78	0.2	sw.gg
3020.6 8			2^+	0.38	0.52	3.72	0.3	sw.gg
3030.3 9			2^+	0.40	0.95	3.83	0.3	sw.gg
3043.0 7			2^+	0.46	0.61	5.91	0.4	sw.gg
3052.4 9			(3^+)	0.51	1.08	3.53	4.2	m2a
3064.3 15			(2^+)	0.48	0.64	2.51	0.1	sw.gg
3072.6 8			(6^+)	0.64	1.20	3.82	0.5	sw.gg
3083.8 7			2^+	0.36	0.64	5.46	0.35	sw.gg
3100.9 7			2^+	0.41	0.58	6.07	0.40	sw.gg
3113.9 12			(≤ 4)	1.04	1.48	2.57		
3124.7 8			(4^+)	0.89	1.15	6.01	1.8	sw.gg
3135.9 10			(≤ 4)	1.42	1.10	4.52	0.7	sw.gg

TABLE II. (*Continued.*)

Level energy (keV)		I^π		Cross-section ratios		σ_{integ} (μb)	Ratio $\sigma_{\text{exp}}/\sigma_{\text{calc}}$	Way of fitting
This work	Refs. [16–18]	Refs. [16–18]	This work	($5^\circ/16^\circ$)	($26^\circ/16^\circ$)			
3147.4 8			(≤ 4)	1.06	0.81	4.65		
3162.0 7			2^+	0.41	0.79	3.44	0.25	sw.gg
3173.6 8			2^+	0.27	0.63	3.29	0.25	sw.gg
3186.1 7			(6^+)	0.46	0.82	2.54	0.4	sw.gg
3198.4 7			2^+	0.63	0.72	3.56	0.1	sw.gg
3212.2 7			2^+	0.50	0.73	2.75	0.08	sw.gg
3223.1 7			2^+	0.54	0.79	3.14	0.08	sw.gg
3234.0 7				0.98	0.89	4.72		
3248.6 7			2^+	0.54	0.72	4.46	0.12	sw.gg
3258.8 8				1.38	1.33	5.09		
3269.9 12			(2^+)	0.85	0.83	4.29	0.12	sw.gg

^aFor the levels at 952.6 and 1125.6 keV the angular distributions can be fitted by the DWBA calculations as spin 1^- or spin 0^+ .

^bFor the levels at 1868.9 and 2422.7 keV the angular distributions are fitted by the DWBA calculations as doublet lines.

The angular distribution for the 0^+ ground state of ^{230}Th has such a shape. This pronounced feature helped us to identify these states in complicated and dense spectra without fitting experimental angular distributions. No complication of the angular distributions was expected, since the excitation of 0^+ states predominantly is a one-step process. This is not the case for the excitation of states with other spins, where multistep processes could play a very important role.

The identification of other states is possible by fitting the experimental angular distributions with those calculated in the DWBA. A problem arising in such calculations is that we have no prior knowledge of the microscopic structure of these states. We can assume, however, that the overall shape of the angular distribution of the cross section is rather independent of the specific structure of the individual states, since the wave function of the outgoing tritons is restricted to the nuclear exterior and therefore to the tails of the triton form factors. To verify this assumption DWBA calculations of angular distributions for different $(j)^2$ transfer configurations to states with different spins were carried out. The coupled-channel approximation (CHUCK3 code of Kunz [19]) was used in these calculations.

The shape of the calculated angular distributions depends strongly on the chosen potential parameters. We used parameters suggested by Becchetti and Greenlees [20] for protons and by Flynn *et al.* [21] for tritons. These parameters have been tested via their description of angular distributions for the ground states of ^{228}Th , ^{230}Th and ^{232}U [3]. They are listed in Table III. Minor changes of the parameters for tritons were needed only for some 3^- states, particularly for the state at 571.7 keV. For these states the triton potential parameters suggested by Becchetti and Greenlees [22] were used (the last column in Table III). For each state the binding energies of the two neutrons are calculated to match the outgoing triton energies. The corrections to the reaction energy are introduced depending on the excitation energy. The best reproduction of the angular distribution for the ground state was obtained for the transfer of the $(2g_{9/2})^2$ configuration in the one-step process. This

orbital is close to the Fermi surface and was considered as the most probable in the transfer process. Other transfer configurations that might be of importance are $(1i_{11/2})^2$ and $(1j_{15/2})^2$, since these orbitals are also near the Fermi surface. All other configurations for the orbitals in the vicinity of the Fermi surface were tested in the one-step calculations. As one can see in Fig. 3, the shape of the angular distributions depends to some degree on the transfer configuration, the most pronounced being found for the 0^+ states. However, the main features of the angular distribution shapes for 2^+ and 4^+ states are not dependent on the transfer configurations. Therefore the $(2g_{9/2})^2$ configuration was used in the calculations for the majority of excited states. For some 0^+ excitations the configurations $(1i_{11/2})^2$ and $(1j_{15/2})^2$ alone or in combination with $(2g_{9/2})^2$ were needed to obtain better reproduction of the experimental angular distributions.

TABLE III. Optical potential parameters used in the DWBA calculations.

Parameters	p	t^a	n	t^b
V_r (MeV)	57.10	166.70		159.0
$4W_D$ (MeV)	32.46			
W_0 (MeV)	2.80	10.28		9.24
$4V_{\text{so}}$ (MeV)	24.80		$\lambda = 25$	
r_r (fm)	1.17	1.16	1.17	1.16
r_D (fm)	1.32			
r_0 (fm)	1.32	1.50		1.50
r_{so} (fm)	1.01			
R_c (fm)	1.30	1.30		1.25
a_r (fm)	0.75	0.75	0.75	0.75
a_D (fm)	0.51			
a_0 (fm)	0.51	0.82		0.82
a_{so} (fm)	0.75			
n_{lc}	0.85	0.25		0.25

^aAccording to Ref. [21].

^bAccording to Ref. [22].

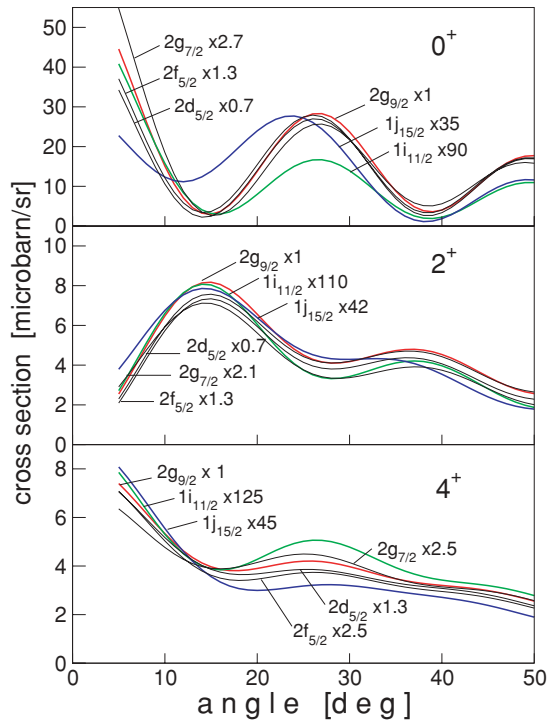


FIG. 3. (Color online) CHUCK3 one-step DWBA calculations of the angular distributions for different $(j)^2$ transfer configurations. The lines are marked with the $(j)^2$ transfer configuration and a scaling factor introduced to allow comparison with the $(2g_{9/2})^2$ transfer configuration.

Results of fitting the angular distributions for the states assigned as 0^+ excitations are shown in Fig. 4. The angular distributions in the two first columns measured with good statistical accuracy are believed to give firm 0^+ assignments. Three possible transfer configurations, $(2g_{9/2})^2$, $(1i_{11/2})^2$, and $(1j_{15/2})^2$, have been used to get the best fit to the experimental data. These configurations are listed in the last column in Table II. The assignments to the states of 1745.3, 2368.5, 2426.4, and 2596.4 keV are considered as relatively firm, because the shape of the angular distribution is fitted perfectly by the calculations, although there is a limited statistical accuracy of the experimental data. The angular distribution for the transition at an excitation energy of 1868.9 keV is fitted as a sum of two angular distributions for transfer to a 0^+ and a 6^+ state (doublet line). A similar situation is assumed for the transition at 2422.7 keV (i.e., a superposition of two angular distributions for 0^+ and 4^+ states). In both cases assignments are tentative.

The angular distributions for energies of 952.6 and 1125.6 keV are a special case. A state with spin 1^- is known at an energy of 951.9 keV; however, the angular distribution of the tritons at an excitation energy of 952.6 keV is completely different from that for a known 1^- state at 508.1 keV. Nevertheless, it can be fitted satisfactorily by an inclusion of one-step and two-step excitations. This angular distribution can also be fitted by a calculation for a 0^+ excitation mainly by the $(1j_{15/2})^2$ transfer configuration with a small admixture of the $(1i_{11/2})^2$ transfer. A spin of

0^+ is assigned to the state with closely lying energy of 927.3 keV in ^{232}U , studied in the α decay of ^{236}Pu [23]. Therefore, we have not excluded spin assignment 0^+ , though the present information is not sufficient to solve the problem. A similar angular distribution is observed for the excitation at 1125.6 keV. But in this case the known level at the closely lying energy of 1127.8 keV has a spin of 3^- . The CHUCK calculations give a satisfactory fit for excitations of the 1^- and 0^+ states but not for the 3^- state. It is interesting to note that the IBM calculations (see the following) predict 0^+ excitations at close energies for both states.

Thus we can make firm spin assignments for 16 states, relatively firm assignments for 4 states, and tentative assignments for 4 others, in comparison with the 14 states found in the preliminary analysis of the experimental data [3].

It is difficult to estimate the additional number of 0^+ excitations above 3 MeV from the spectra at 12.5° and 26° in Fig. 2. The intensities of the lines corresponding to 0^+ states have to be very low for 12.5° and much higher for 26° . The lines fulfilling this condition are labeled by their energies. Unfortunately, a similar condition is fulfilled also for 6^+ excitations as well as for less probable 2^- and 3^+ states. To be sure of the presence of 0^+ states in this high-energy region at least a spectrum for the most forward angle has to be measured. But there is an impression from the measured spectra that the density of 0^+ states decreases for energies above 3 MeV (or else that the cross section of such excitations is very low and they are hidden in very dense and complicated spectra). The maximum density of 0^+ states is observed in the interval between 2 and 3 MeV, as one can see in Fig. 5. The neutron pairing gap for ^{230}Th is about 750 keV and this leads to two-quasiparticle excitations around 1.5 MeV. Thus the maximum density of 0^+ states above this energy may be caused by inclusion of such excitations, as predicted by the calculations [24].

Similar to 0^+ excitations, the one-step transfer calculations give a satisfactory fit of angular distributions for about 70% of the states with spins different from 0^+ but about 30% of these states need the inclusion of multistep excitations. Multistep excitations have to be included to fit the angular distributions already for the 2^+ , 4^+ , and 6^+ states of the ground-state band. Figure 6 shows the schemes of the multistep excitations tested for every state in those cases where one-step transfer does not provide a successful fit. Figure 7 demonstrates the quality of the fit of some different-shaped angular distributions for the excitation of states with spins higher than 0^+ by calculations assuming one-step and one-step plus two-step excitations. The fits for the ground-state band are included in Fig. 7. Whereas natural parity states can be populated by one-step or one-step plus two-step mechanisms, the states of unnatural parity can be excited only by two-step excitations. The angular distributions and their fits for such excitations are presented in Fig. 8.

The assignments of the spins resulting from such fits are presented in Table II together with other experimental data. Detailed explanations of this table are given in Sec. II A. Special comments are needed for the column displaying the ratio $\sigma_{\text{exp}}/\sigma_{\text{calc}}$. Since we have no *a priori* knowledge of microscopic structure of the excited states and thus we do not know the relative contributions of the specific $(j)^2$

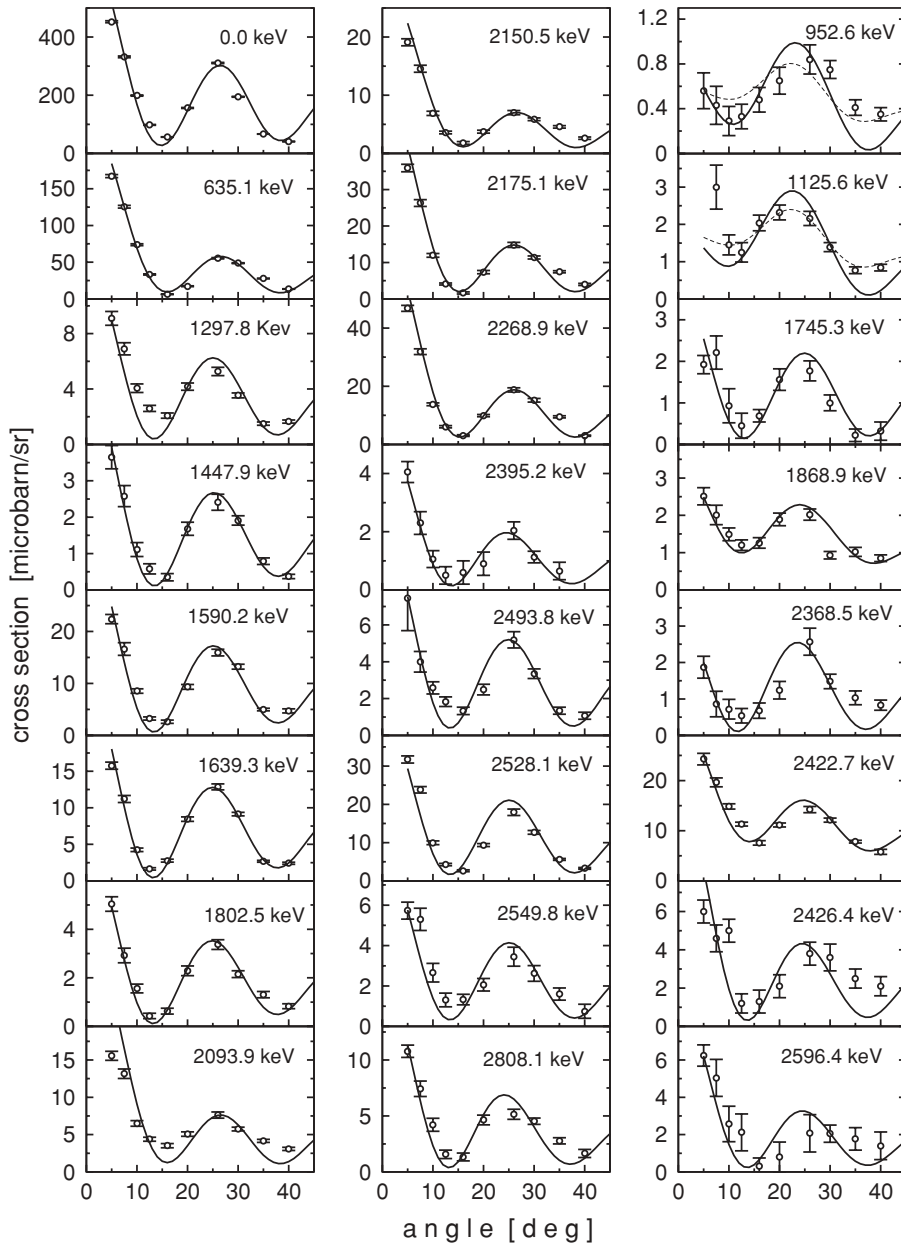


FIG. 4. Angular distributions of assigned 0^+ states in ^{230}Th and their fit with CHUCK3 one-step calculations. The (ij) transfer configurations used in the calculations for the best fit are given in Table II. The first two columns on the left correspond to firm assignments and the column on the right to tentative assignments.

transfer configurations to each of these states, these ratios cannot be considered as spectroscopic factors. Nevertheless, a very large ratio, such as in the case of the $(1i_{11/2})^2$ transfer configurations used in the calculation for the 0^+ state at 635 keV, is unexpected.

Some additional comments on Table II are needed. There are some contradictions in the assignment of the energy of the second 4^+ level. It has been proposed from Coulomb excitation to be at 772.1 keV in Ref. [25] and at 769.6 keV in Ref. [26] and from the $(d, p\eta\gamma)$ reaction at 775.5 keV [18]. The value 769.6 keV is accepted in the compilation of Ref. [16]. We see a weak peak at 775.2 keV on the tail of the very strong peak at 781.4 keV as confirmation of the 775.5-keV assignment [18]. There is not even a hint of a peak at 769.6 keV. Again the 8^+ and 10^+ levels proposed in Ref. [26] at 1251.4 and 1520.4 keV (both accepted in the compilation of Ref. [16]) are in contradiction with the assignment of the

8^+ level at 1243.2 keV and with the calculated energy of the 10^+ level at 1487 keV [18]. The (p, t) study confirms the assignment for the 8^+ level at 1243.2 keV by the observation of a weak peak at 1241.2 keV and no peak in the vicinity of 1251.4 keV. After this confirmation the smooth change of the inertial parameter in the band prefers an energy of 1487 keV for the 10^+ level and rejects the energy of 1520.4 keV.

There are several levels in ^{230}Th for which spins 1^- , 2^+ or $1, 2^+$ were assigned from the β^- decay and/or inelastic scattering and for which the (p, t) angular distributions are measured: 1573.5, 1695.7, 1770.7, 1839.6, 1849.6, 1966.9, 1973.4, 2000.9, 2010.1, and 2024.7 keV (with energies from the compilation of Ref. [16]). Angular distributions from the (p, t) reaction confirm spin 2^+ for some of them: 1840.0, 1967.1, 1972.0, 2010.3, and 2025.6 keV [energies as determined from the (p, t) reaction]. The (p, t) angular distributions for other states cannot be fitted for the spins given

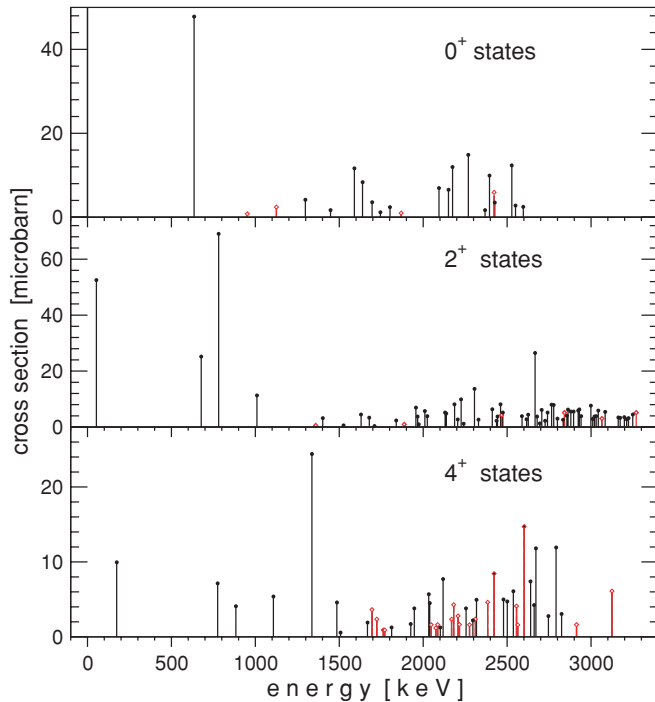


FIG. 5. (Color online) Experimental distribution of the (p,t) strength integrated in the angle region $0^\circ\text{--}45^\circ$ for 0^+ , 2^+ , and 4^+ states in ^{230}Th . The levels identified reliably are indicated by filled circles and those identified tentatively are indicated by open diamonds.

in Ref. [16]. If the energies of 1574.5(6) keV from the (p,t) reaction and 1573.5(2) keV from Ref. [16] correspond to the same level, then a different assignment is suggested by the (p,t) angular distribution to this state as 2^- or 3^+ . In any case, a 2^+ excitation would manifest itself in the (p,t) angular distribution and therefore has to be excluded. For the states at 1694.9 and 1769.6 keV we observe angular distributions that can be fitted by calculations for 4^+ states (or even for a 0^+ state plus a constant of about $2 \mu\text{b}$ for the state of 1694.9 keV). Either way, the assignment 2^+ can be excluded. Finally, the (p,t) angular distributions for the states at 1851.4 and 2001.6 keV prefer an assignment of 3^- in contradiction to (2^+) and 1, 2^+ , respectively, as given in Ref. [16].

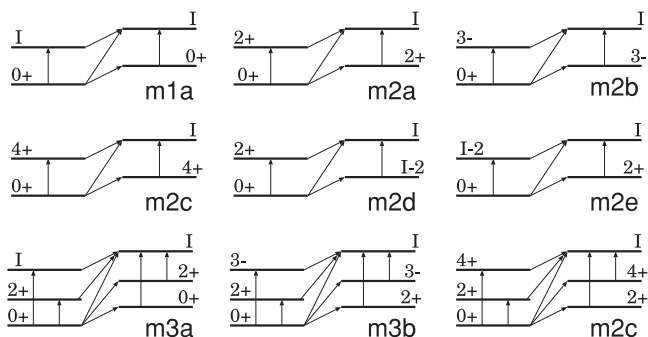


FIG. 6. Schemes of the CHUCK3 multistep calculations tested with spin assignments of excited states in ^{230}Th (see Table II).

C. Collective bands in ^{230}Th

After the assignment of spins to all excited states the sequences of states can be distinguished, showing the characteristics of a rotational band structure. An identification of the states attributed to rotational bands was made on the following conditions:

- (i) the angular distribution for a state as band member candidate is fitted by the DWBA calculations for the spin necessary to put this state in the band;
- (ii) the transfer cross section in the (p,t) reaction to the states in the potential band has to decrease with increasing spin; and
- (iii) the energies of the states in the band can be fitted approximately by the expression for a rotational band $E = E_0 + AI(I + 1)$ with a small and smooth variation of the inertial parameter A .

Collective bands identified in such a way are shown in Fig. 9 and are listed in Table IV (for a calculation of the moments of inertia). The procedure can be justified in that some sequences meeting these criteria are already known from γ -ray spectroscopy to be rotational bands, so other similar sequences are very probably rotational bands too. The straight lines in Fig. 9 strengthen the argument for these assignments. For example, the mean deviation of the experimental energies from the calculated rotational values for the longest newly assigned band based on the state 0^+ at 1589 keV is only 1.0 keV; for the band based on the 0^+ state at 2093.9 keV it is 1.3 keV; and for the band above the 0^+ state at 2268.9 keV it is 3.9 keV. Even for the band above the 0^+ state at 2426.4 keV assigned tentatively the deviation is less than 1 keV. The observed deviations are all consistent with the stretching effect typical for rotational bands. Nevertheless, additional information (on $E2$ transitions at least) is needed to confirm these assignments.

It is worth mentioning that the tentative assignment 0^+ for the state at 2426.4 keV is supported by a sequence of three other states (2^+ , 4^+ , and 6^+) on top of it. Three other tentative 0^+ states (1745.3, 1868.9, and 2422.7 keV) have only one tentative state (2^+) on top of them and the band sequence is not based on γ -ray transitions but on energy arguments. In Table V we present moments of inertia (MoI) obtained by fitting the level energies of the bands displayed in Fig. 9 by the expression $E = E_0 + AI(I + 1)$. The upper part of the table presents those sequences that are connected by known γ -ray transitions or have at least three levels; the lower part of the table presents the sequences having only two levels or being tentatively assigned. The obtained MoI cover a broad range from ~ 50 to $\sim 100 \text{ MeV}^{-1}$. The negative-parity bands based on the states with spin 1^- interpreted as the octupole-vibrational bands [18] have high MoI (with the 1^- band at 951 keV having the largest MoI). The 0^+ band at 1297 keV, considered as a β -vibrational band, has the smallest MoI. At this stage, it is difficult to make a complete correlation between the intrinsic structure of the bands and the magnitude of their MoI. Nevertheless, one can assume also for the 0^+ bands that the largest MoI could be related to the octupole phonon structure and the smallest MoI could be related to the one-phonon quadrupole structure. The

TABLE IV. The sequences of states qualifying as candidates for rotational bands (from the CHUCK fit, the (p,t) cross sections, and the inertial parameters). More accurate values of energies are taken from the first two columns of Table II. The energies given in parentheses correspond to the sequences assigned tentatively.

0 ⁺	1 ⁺	2 ⁺	3 ⁺	4 ⁺	5 ⁺	6 ⁺	7 ⁺	8 ⁺	
0.0		53.2		174.0		356.3		593.8	
634.9		677.5		775.5		923.0		1117.5	
		781.4	825.6	883.9	955.1	1039.6	1134.2	1243.3	
		1009.6	1052.3	1107.5	1176.1	1255.5	1349.3	1448.7	
1297.1		1359.5		1507.4					
				1337.2		1496.0			
1447.9		1524.8							
1589.8		1630.1		1723.5		1868.9		2073.2	
1638.5		1679.1		1770.7		1910.0			
(1744.9)		1789.4							
1802.5		1839.6		1926.0					
(1868.9)		1902.7							
		1956.4	1985.4	2048.7		2194.8			
		1966.9		2074.9		2249.9			
		2010.1		2102.0		2249.9			
2093.9		2130.7		2216.0		2354.8			
2150.5		2187.1		2276.0		2402.0			
2175.1		2205.4		2276.0		2388.4			
		2226.0		2317.7		2481.3			
2268.9		2305.4		2383.8		2519.3			
(2422.7)		2474.3							
				2422.7		2573.2			
(2426.4)		2467.2		2562.9		2712.9			
		2411.6		2501.1					
		2461.0		2556.2					
2528.1		2589.1		2746.2		2950.5			
2549.8		2616.0							
		(2666.0)		2791.5		2987.9			
2808.1		2841.3		2913.6					
		2999.0		3124.7					
	1 ⁻	2 ⁻	3 ⁻	4 ⁻	5 ⁻	6 ⁻	7 ⁻	8 ⁻	9 ⁻
	508.2		571.7		686.7		851.9		1065.9
	951.9	972.1	1012.5	1065.9	1109.0				
		1079.4	1127.8	1196.8	1283.6				
			(1259.2)		1376.7				
	(1789.4)		1858.6		1985.4				
	(1775.2)		1849.6		1985.4				
	(1931.1)		2000.9		2133.2				
	(1939.8)		2017.3						

bands with intermediate values of MoI could be based on the two-phonon quadrupole excitations.

If the moments of inertia do indeed carry information on the inner structure of the bands, then the numbers of excitations with different structure are comparable. This would be in contradiction with the IBM calculation, which predicts predominantly the octupole two-phonon structure of 0⁺ excitations (see the following). The nature of 0⁺ excitations, derived from calculations in the framework of the QPM as predominately quadrupole, is in contradiction with both the IBM calculation and with these empirical observations (see the following).

D. Excited states with spins higher than 0⁺

Other states, mainly with spins of 2⁺, 4⁺, and 6⁺, are intensively excited in the (p,t) reaction. The nature of these states may only be assumed. Some of these states could belong to the collective bands based on 0⁺ states. Some of the 2⁺ states could be quadrupolar (one-phonon) vibrational states with correspondence to 0⁺ excited states, since in deformed nuclei every excitation of angular momentum I^π splits into states distinguished by their K quantum numbers ranging from 0 to I . Some 4⁺ excited states could be hexadecapole vibrational excitations and 2⁺ and 0⁺ states should correspond to this class of states for the same reason. If this speculation reflects reality

TABLE V. Moments of inertia for the bands in ^{230}Th as assigned from the angular distributions from the $^{232}\text{Th}(p,t)^{230}\text{Th}$ reaction. Results derived from the sequences having only two levels or assigned tentatively are given in the lower part of the table.

E (keV)	$J(0^+)$	E (keV)	$J(2^+)$	E (keV)	$J(1^-, 3^-)$
0.0	56.8	781	67.5	508	78.3
635	70.1	1009	70.0	951	98.5
1297	47.8	1956	62.9	1079	61.7
1589	74.0	1967	64.5	1259	79.4
1639	75.7	2010	75.7	1789	72.0
1802	80.5	2226	76.0	1931	71.3
2093	81.2	2666	55.5		
2150	81.6				
2175	98.5				
2269	81.8				
2426	74.0				
2528	49.0				
2808	89.5				
1448	40.0	2412	78.0	1259	79.4
1745	67.2	2461	73.1		
1868	88.4	2999	55.4		
2422	58.0				
2550	45.7				

then the number of 0^+ states has to be the largest. However, the observation is in contradiction with this conjecture unless very weak 0^+ excitations are not seen in the (p,t) reaction. Attributing the underlying structure to each of the observed states is not possible with the presently available experimental data. To give at least a hint for the structure of these states the experimental energy distribution of the (p,t) transfer strength for the 0^+ , 2^+ , and 4^+ excitations is plotted in Fig. 5.

A most remarkable feature in Fig. 5 is the most strongly excited 4^+ state at 1337 keV, which can be related to the strongly excited 0^+ state at 635 keV and 2^+ state at 781 keV. The inertial parameters derived from the bands based on these states are practically the same. The only explanation is that these states have the same structure. One can assume that these states are a triplet originating from an excitation of multipolarity 4 as in the case of a quadrupole two-phonon excitation. However, corresponding strongly excited one-phonon quadrupole excitations with spins 0^+ and 2^+ are not observed at lower energy. Indeed, the 0^+ state at 1297 keV, which was identified as the β -vibrational state [18], is rather weak. Thus quadrupole two-phonon excitations have to be excluded. On the assumption that these states have a two-phonon octupole structure a quadruplet of states has to be observed with spins from 0^+ to 6^+ . Experimentally, a state with spin 6^+ is identified at 1653 keV, although its excitation is only $0.9 \mu\text{b}$ (i.e., much weaker than the other states). If this assumption is correct, then the interpretation of the first 0^+ state as a two-phonon excitation becomes somewhat confirmed. This quadruplet of states and the corresponding bands are displayed in Fig. 10. Note, however, that the moments of inertia derived from the band based on the states of the multiplet are somewhat smaller than the ones derived for the bands based on negative-parity states (Table V).

An indirect confirmation of this assumption would be the existence of another quadruplet. The 1^- levels at 508 and 952 keV and the 2^- level at 1079 keV were interpreted as members of a quadruplet of octupole shape oscillations with $K^\pi = 0^-$ to 3^- [18]. The 3^- level at 1259 keV identified from the (p,t) reaction in the present study can be the missing member of this quadruplet, as shown in Fig. 10. The energy separation between the $K^\pi = 0^-$ and $K^\pi = 1^-$ and between the $K^\pi = 1^-$ and $K^\pi = 2^-$ bandheads differs strongly. This was explained by a strong coupling of the bands based on the last two states [18]. The energy separation between the 3^- level at 1259 keV and the 2^- level is close to the one between the second 1^- and 2^- levels, which can also be attributed to the coupling of these three states.

III. DISCUSSION

A. 0^+ excitations

The importance of pairing in the enhancement of the cross section of the 0^+ two-nucleon transfer reaction was noted already in an earlier publication [27,28]. The superfluid ground states of deformed nuclei are strongly populated in the (p,t) reaction owing to the large overlap of the wave functions between nuclei with neutron number N and $N \pm 2$. The excited 0^+ states can be populated in the (p,t) reaction by the fluctuation of the pairing field. Such states represent pairing vibration modes [27,28]. It was realized that pairing correlations in deformed nuclei are induced not only by monopole but also by quadrupole pairing interactions. If both pairing fields are comparable in strength and if there is a nonuniform distribution of oblate and prolate single-particle orbitals around the Fermi surface, this may give rise to 0^+ excitations treated as pairing isomers decoupled from the deformed superfluid ground state [24,29]. An asymmetry between (p,t) and (t,p) cross sections predicted by this model was confirmed in an experiment by Casten *et al.* [30].

The structure of excited 0^+ states in deformed even-even nuclei is still a matter of controversial discussion despite intensive investigation. Traditionally, the first excited 0_2^+ state has been interpreted as the β -vibrational excitation of the ground state. However, in many nuclei the 0_2^+ state has only weak transitions to the ground-state band, whereas strong electric quadrupole transitions to the γ band have been found [31]. This contradicts the traditional interpretation, since a transition from a β -vibrational state to the γ band is suppressed by the destruction of a β phonon and, at the same time, the creation of a γ phonon. The unclear situation led to an intense debate about the structure of low-lying 0^+ states.

Maher *et al.* [2] were the first who noticed an interesting feature of 0^+ excited states in the actinides. The strong excitations of the first excited 0^+ states in the (p,t) reaction, combined with all other available evidence (rather weak $E2$ transitions to the ground-state band, strong α decays leading to them, and the strong Coulomb excitation of the associated collective bands) suggest that these states represent a new and stable collective excitation, different in character from the most common formulation of the pairing vibration as well as from the β vibration usually found in the deformed

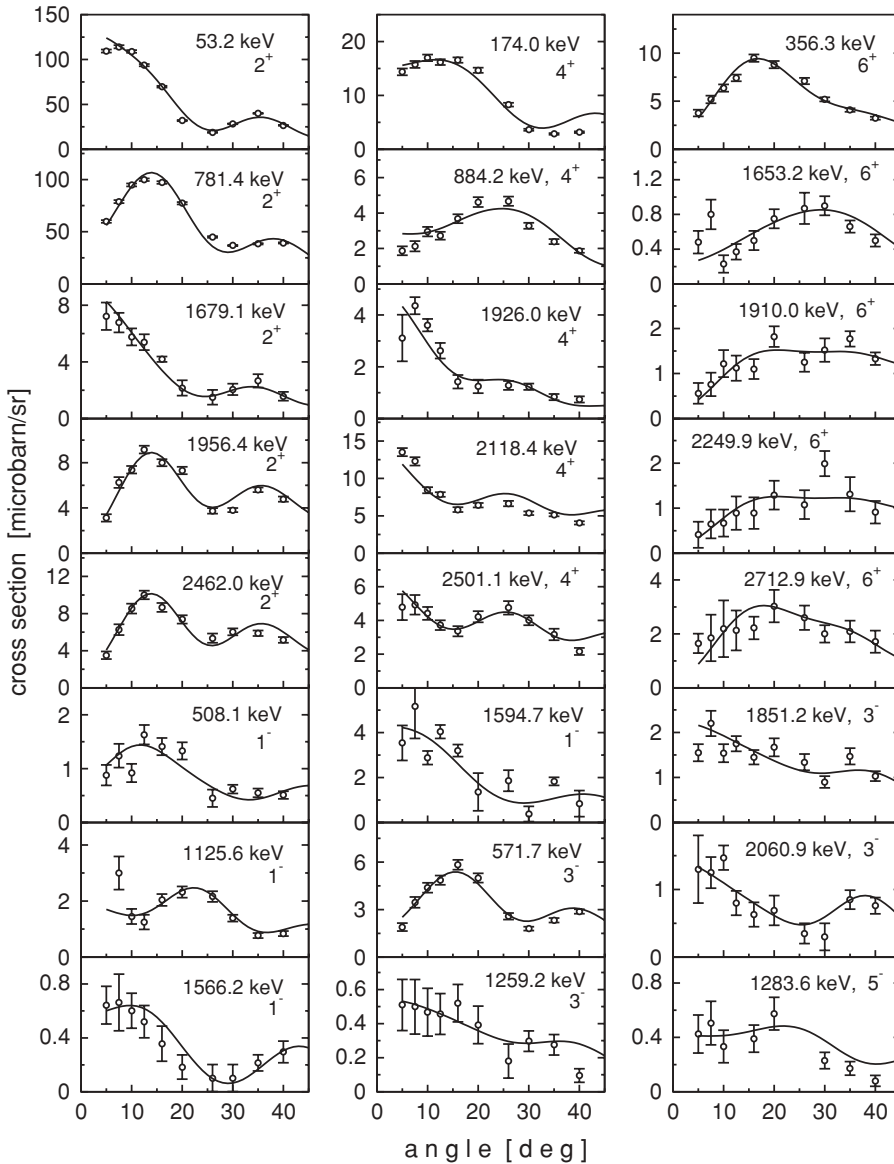


FIG. 7. Angular distributions of some excited states of natural parity and their fit by the CHUCK3 calculations. The (ij) transfer configurations and schemes used in the calculations for the best fit are given in Table II.

rare-earth nuclei. The second excited 0^+ states in actinides (firmly assigned) demonstrate completely different features [18,32,33]. Weak excitation in the (p,t) reaction, relatively strong $E2$ transitions to the ground-state band, and a small $B(E1)/B(E2)$ ratio for transitions to 2^+ and 1^- states give evidence that they could be the usual β vibrational states. For ^{230}Th this is the case for the level at 1297.8 keV [18]. Otsuka and Sugita [34] applied the $spdf$ -IBM to the actinide nuclei, aiming to get a unified description of quadrupole-octupole collective states. They suggested the first excited 0^+ band be referred to as the “super β band,” thus emphasizing the difference of the structure of this state from that of the usual β -vibrational state. They also predicted the existence of the second excited 0^+ band to be the usual β band that was confirmed later. There is evidence for the first 0^+ state in ^{230}Th (quadruplet of states and large moment of inertia comparable to that for the octupole-vibrational bands, together with the aforementioned features noticed by Maher *et al.* [2]) to carry the two-phonon octupole nature. However, the $B(E1)/B(E2)$

ratio for transitions to the 1^- and 2^+ states is even smaller for this state than for the state at 1297 keV: $\sim 4 \times 10^{-7} \text{ fm}^{-2}$ compared to $\sim 7 \times 10^{-7} \text{ fm}^{-2}$ [18]. Intuitively, one would expect that a large $B(E1)/B(E2)$ ratio might be characteristic for a two-octupole-phonon excitation, whereas a small ratio might indicate a β shape oscillation. That is true for the state at 1297 keV (which indeed is a β -vibrational state), but it is not true for the first excited state. Moreover, the IBM and the QPM predict a one-phonon quadrupole nature for this state (see the following). Therefore the available data do not allow the firm conclusion on the nature of this state.

Understanding of the structure of the higher excited states remains a challenge for further experimental studies [e.g., γ spectroscopy in the $(p,t\gamma)$ reaction] and for nuclear theory. The first attempt to explain experimental data of a large number of 0^+ excited states in ^{158}Gd [35] was a phenomenological approach [36] based on the extended interacting boson model ($spdf$ -IBM), which accounted for a large fraction of the observed states. The importance of the octupole degrees of

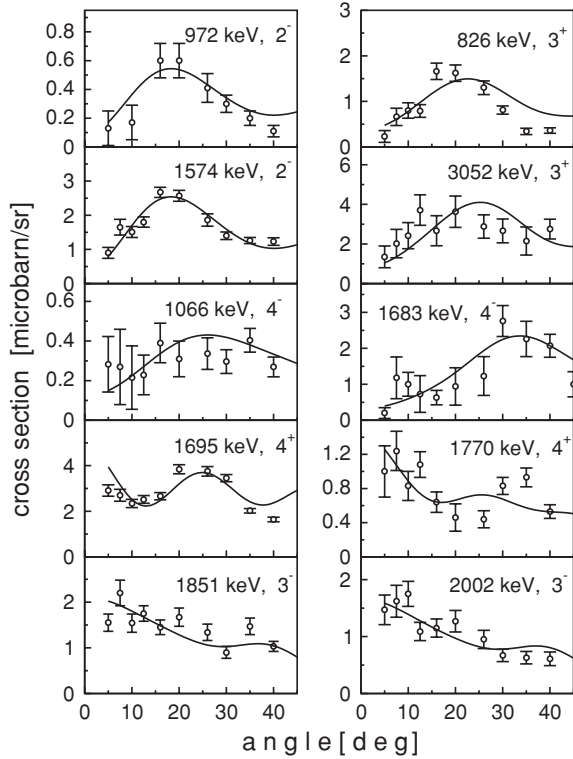


FIG. 8. Angular distributions and their fit by the CHUCK3 calculations for some excited states of unnatural parity and for the states where our assignments of spins are in contradiction with the compilation of Ref. [16]. The (ij) transfer configurations and schemes used in the calculations for the best fit are given in Table II.

freedom was revealed. The first microscopic approach was performed in the framework of the projected shell model (PSM) [37], using a restricted space spanned by two and four quasiparticle states. The IBM calculation reproduced satisfactorily all energy levels in ^{158}Gd and gave small $E2$ decay strengths for them. Soloviev and co-workers [38,39] applied the QPM to get a microscopic understanding of low-lying 0^+ states. The QPM was also applied to ^{158}Gd [40]. It predicts a sizable fraction of the 0^+ states to have large or dominant two-phonon components, mainly built from collective octupole phonon components, in agreement with the IBM calculations [36].

The results of a specific analysis of experimental data for actinide nuclei were compared to the *spdf*-IBM calculations in our previous paper [3]. After publication of these data, Lo Iudice *et al.* carried out a calculation for these nuclei in the framework of the QPM [41]. Although energies, $E2$ and $E0$ transition strengths, and two-nucleon transfer spectroscopic factors were computed, only some of them could be compared with the then available experimental data. We compare our new data for ^{230}Th with the results of both calculations here.

No extended calculations have yet been carried out for the excitation of the two-quasiparticle (2QP) modes, which are expected to occur at excitation energies of about twice the pairing gap energy (i.e., about 1.5 MeV in our case). Only very restricted microscopic calculations for low energies were attempted by Ragnarsson and Broglia [24]. It would be

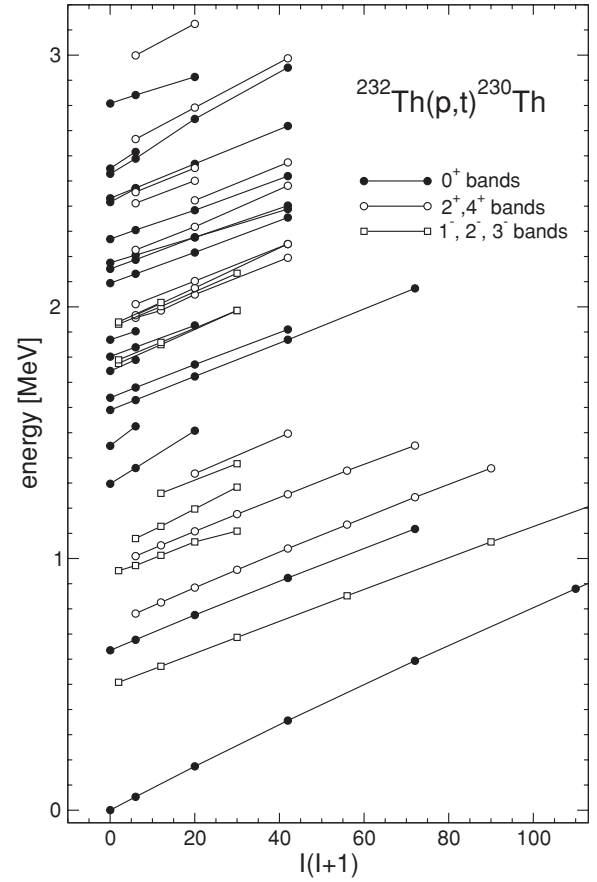


FIG. 9. Collective bands based on the 0^+ , 2^+ , 4^+ , 1^- , 2^- , and 3^- excited states in ^{230}Th as assigned from the DWBA fit of the angular distributions from the (p,t) reaction.

desirable to extend these calculations to higher energies. Just above 1.5 MeV, exactly in the range 2.0–2.5 MeV, a bump in the distribution of the (p,t) transfer strength is observed (Fig. 5). At least some of these excitations could be of 2QP nature. A model by van Rij and Kahana [42] describing the 0^+ state as a pair of holes in the oblate $1/2[501]$ Nilsson level should also be mentioned.

The monopole pairing vibration state for neutron-pair excitation (n -MPV) is expected to be strongly excited in the (p,t) reaction because of the large overlap of the wave function of such a state with that of the target nucleus ground state. A dominant (p,t) cross section for a single state in the spectrum (besides the ground and the first excited states) is observed in some nuclei. In ^{229}Pa the cross section for the $L = 0$ transfer to the state at 1500 keV is about 15% of that for the ground state and comparable to that for the first excited 0^+ state in ^{230}Th [4]. However, this behavior is unexpected, since this energy corresponds more to that of the proton-pair excitation (p -MPV), where the cross section is expected to be much weaker. At the same time, a dominant cross section in ^{228}Th is observed for a single state at about 2.1 MeV, much higher than in ^{229}Pa , which can be considered as being due to the ^{228}Th core plus a proton. These facts, as well as practically no correspondence of the energy distribution of the (p,t) strength in these two nuclei, need a theoretical explanation.

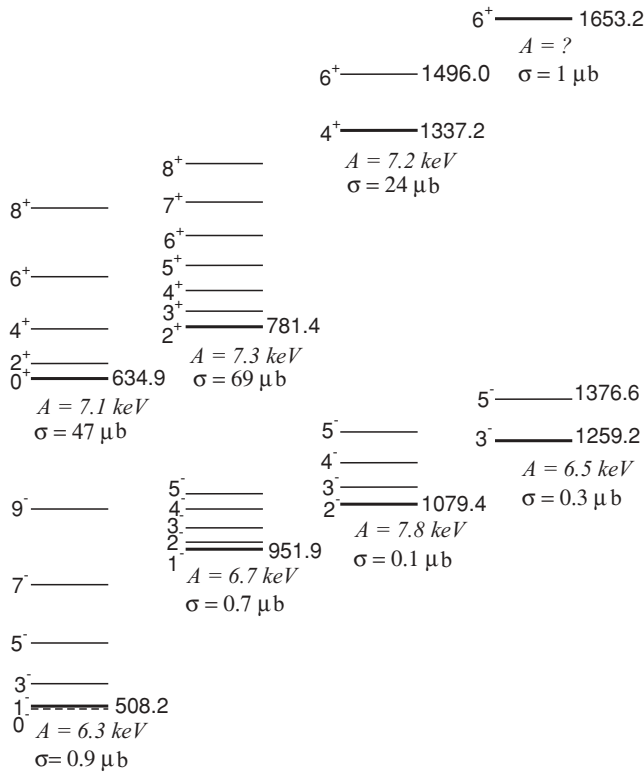


FIG. 10. Assumed multiplets of states of the octupole one-phonon (bottom) and the octupole two-phonon (top) excitations and corresponding collective bands.

No dominant excitation at higher energies is observed in ^{230}Th . In the case of a relatively dense spectrum of 0^+ states, fragmentation of the n -MPV state to nearby states is possible. Such a group of states in ^{230}Th around 1600 keV could be a result of such fragmentation. The summed cross section of this group is about 13% of that for the ground state. A similarly dense spectrum occurs also in ^{228}Th and ^{229}Pa ; nevertheless, these nuclei demonstrate dominant excitation of individual states. Unfortunately, no calculations have been carried out for odd nuclei, though they are planned for ^{229}Pa [43]. There is no clear picture concerning the problem of the MPV as well as of the 2QP states.

B. IBM calculations

Although ^{230}Th is considered a vibrational-like nucleus, the inclusion of the octupole degree of freedom in the description of its properties turned out to be important [18]. The role of the octupole degree of freedom in deformed actinide nuclei and the related description with f bosons added to the IBM in the sd boson space (sd -IBM) has been studied in Ref. [44]. Despite reproducing reasonably well the main features of the observed low-lying negative-parity states in the rare-earth nuclei [45], the sd -IBM was not so successful for the actinide nuclei. A better reproduction of the relevant data is obtained if a p boson is included in addition to the f boson without seeking an understanding of its physical nature [46].

The IBM Hamiltonian in the $spdf$ space includes a vibrational contribution and a quadrupole interaction in the

simple form [36,46]

$$H = \epsilon_d \hat{n}_d + \epsilon_p \hat{n}_p + \epsilon_f \hat{n}_f - \kappa \hat{Q}_{spdf} \cdot \hat{Q}_{spdf}, \quad (1)$$

where ϵ_d , ϵ_p , and ϵ_f are the boson energies and \hat{n}_d , \hat{n}_p , and \hat{n}_f are the boson number operators. Note that the same strength κ of the quadrupole interaction describes the sd bosons and the pf bosons. The \hat{Q}_{spdf} quadrupole operator has the form

$$\begin{aligned} \hat{Q}_{spdf} = & \hat{Q}_{sd} + \hat{Q}_{pf} = [s^\dagger \tilde{d} + d^\dagger s]^{(2)} \\ & - \chi_{sd} [d^\dagger \tilde{d}]^{(2)} + (3/5) \sqrt{7} [p^\dagger \tilde{f} + f^\dagger \tilde{p}]^{(2)} \\ & - (9/10) \sqrt{3} [p^\dagger \tilde{p}]^{(2)} - (3/10) \sqrt{42} [f^\dagger \tilde{f}]^{(2)}. \end{aligned} \quad (2)$$

The factor in front of the $[d^\dagger \tilde{d}]^{(2)}$ term may be adjusted by introducing an additional parameter χ_{sd} .

The IBM parameters in the sd boson space are determined by the low-energy spacing of the ground-state band and the $I^\pi = 2_1^+$, $K^\pi = 0^+$ and $I^\pi = 2_1^+$, $K^\pi = 2^+$ bandheads, respectively. The pf boson parameters are chosen to reproduce the $K^\pi = 0^-$ and $K^\pi = 1^-$ bandheads; they are determined by the experimental energies of the $I^\pi = 1_1^-$, $K^\pi = 0^-$ and $I^\pi = 1_2^-$, $K^\pi = 1^-$ states. The total number of bosons is 11. The number of negative-parity bosons is allowed to range from 0 to 3. Relative to the calculations presented in our earlier paper [3], only some parameters are slightly changed in the present calculations: $\epsilon_p = -1.00$, $\epsilon_d = 0.25$, $\epsilon_f = -0.90$, $\kappa = -0.014$, and $\chi_{sd} = -1.00$. As for rare-earth nuclei [36], in the $spdf$ -IBA calculations mixing between d and pf bosons is neglected and the f (and p) bosons account for octupole collectivity. In Fig. 11 we display the firmly assigned

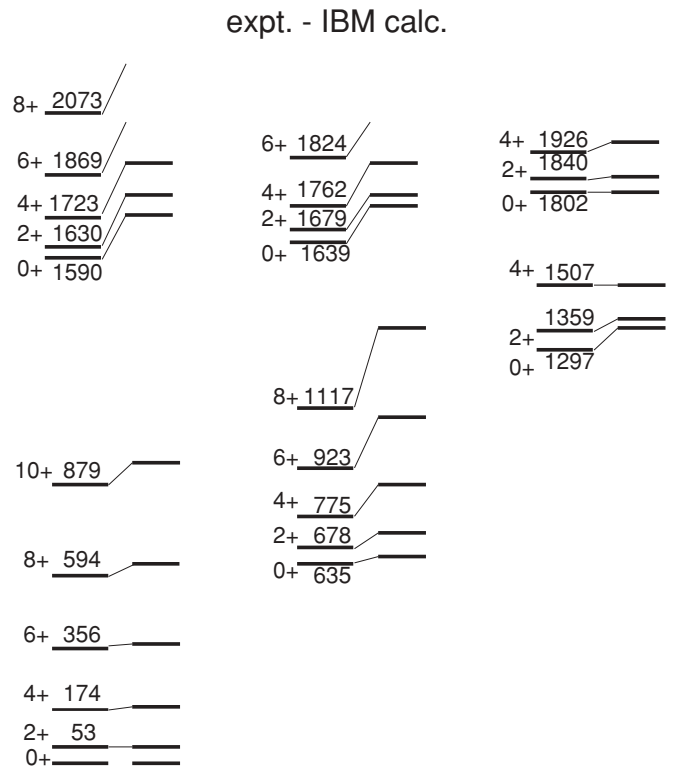


FIG. 11. Lowest 0^+ bands identified earlier and suggested in this analysis in comparison to the $spdf$ -IBM calculations.

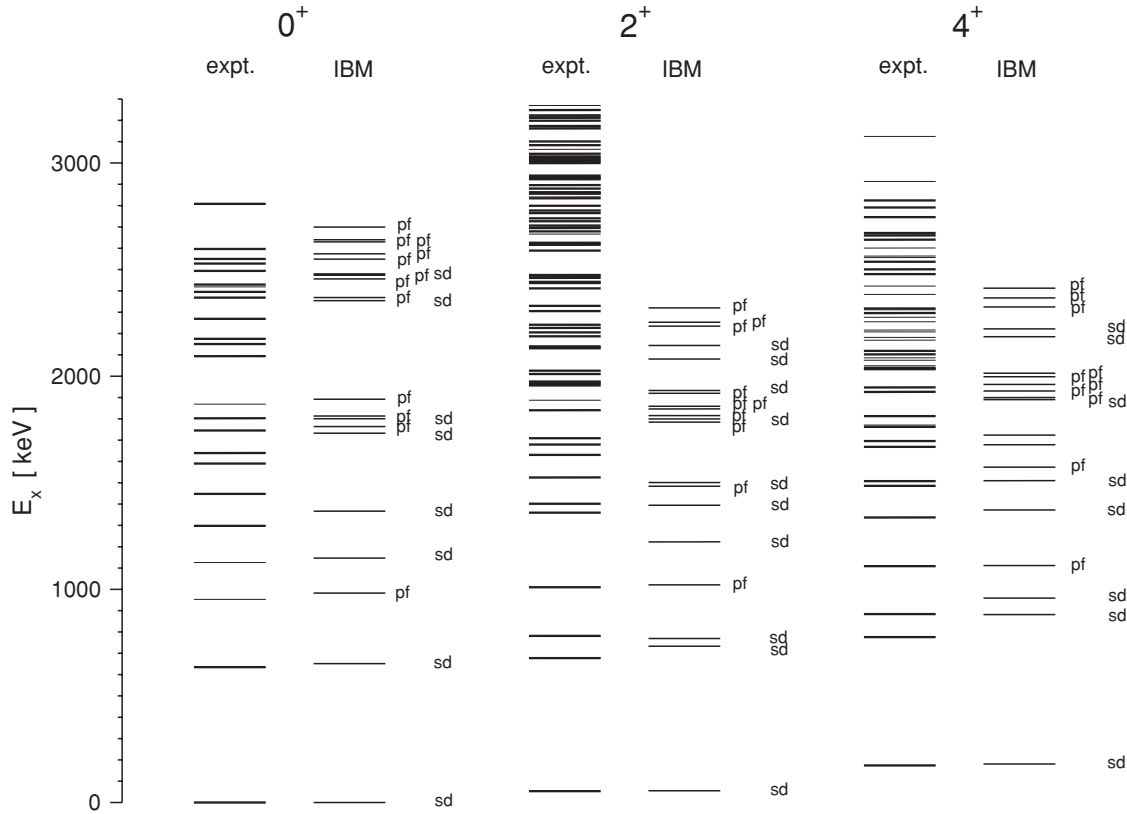


FIG. 12. Energies of all experimentally assigned excited 0^+ , 2^+ , and 4^+ states in ^{230}Th in comparison with *spdf*-IBM calculations. The structure of the states derived from calculations is indicated to the right of the corresponding lines. The firmly assigned states are shown by thick lines; tentatively assigned states are indicated by thin lines.

experimental 0^+ states and the sequences on top of them, in comparison with the *spdf*-IBM calculations.

The full experimental spectrum of the 0^+ states in ^{230}Th , including relatively firm and tentative assignments, and the results of *spdf*-IBA calculations are compared in Fig. 12. In the energy ranges covered experimentally, the IBM predicts 7 excited 0^+ states of pure *sd* (quadrupolar) bosonic structure and 12 excited 0^+ states that have two bosons in the *pf* boson space. They could be related to octupole two-phonon (OTP) excitations. The nature of the states according to the calculations is indicated in Fig. 12. The number and the nature of the 0^+ states in the IBM calculations depend on the parameter values but the solution presented in Fig. 12 is stable for a realistic variation of these parameters. A complete study of these dependencies would be instructive but it is not the goal of the present paper.

We can see a reasonable correlation in excitation energy between experiment and calculation up to 1.4 MeV. The calculation predicts the first excited 0^+ state as a quadrupole excitation in the *sd* space at an energy close to the experimental state at 635 keV. The second excited 0^+ state is predicted as an OTP excitation and could correspond to the tentative assigned 0^+ state at 953 keV. The following two are predicted to have a quadrupole structure and correspond energetically to the tentative assigned 0^+ state at 1126 keV and to the 0^+ state at

1297 keV, respectively. The latter was, indeed, considered the β -vibrational state in Ref. [18].

Thus the IBM calculation with the parametrizations used predicts for ^{230}Th 20 excited 0^+ states in the energy range below 2.7 MeV. Accounting in addition for the presence of monopole pairing vibrational states, two-quasiparticle states, and perhaps a state from hexadecapole collectivity, not included in the calculation, we can consider 24 observed 0^+ excitations as nearly perfect agreement with the calculated number of such excitations. But there is no clarity concerning the nature of these excitations without additional experimental information. The IBM also fails to completely reproduce the (p,t) spectroscopic factors. The calculated first excited 0^+ state occurs with about 1% of the transfer strength of the ground state, and the higher states are even weaker, whereas experimentally the excited states show at least about 70% of the ground-state transfer strength.

A calculation in the framework of the *spdf*-IBM gives 20 levels of spins 2^+ , 4^+ , and 6^+ , in comparison with 40, 32, and 11 identified levels of these spins in the energy region below 2.7, 2.3, and 2.4 MeV, respectively. The spectrum of 2^+ and 4^+ states in comparison with the *spdf*-IBM calculation is given in Fig. 12. Most of the 6^+ states could not be observed in the (p,t) reaction because of their low cross section. As far as 2^+ and 4^+ states are concerned, the number

of experimental levels is much higher than the prediction of the *spdf*-IBM.

C. QPM calculations

The ability of the QPM to describe multiple 0^+ states (energies, $E2$ and $E0$ strengths, and two-nucleon spectroscopic factors) was demonstrated for ^{158}Gd [40]. An extension of the QPM to describe the 0^+ states in the actinides [41] was made after our publication on the results of a preliminary analysis of the experimental data [3]. The present calculations aim to explain the results of the detailed analysis of the experimental data for ^{230}Th .

In the QPM [47] the Hamiltonian in a separable generalized form is adopted to generate the QRPA phonons described by the operators

$$Q_{iv}^\dagger = \frac{1}{2} \sum_{q_1 q_2} (\psi_{q_1 q_2}^{iv} \alpha_{q_1}^\dagger \alpha_{q_2}^\dagger - \phi_{q_1 q_2}^{iv} \alpha_{q_2} \alpha_{q_1}). \quad (3)$$

The Hamiltonian expressed in terms of these phonon operators is diagonalized in the space spanned by one- and two-phonon states. The QPM eigenstates have the structure

$$\Psi_{nK} = \sum_i C_i^{(n)} Q_{i\lambda K}^\dagger |0\rangle + \sum_{v_1 v_2} C_{v_1 v_2}^{(n)} [Q_{v_1}^\dagger \otimes Q_{v_2}^\dagger]_K |0\rangle, \quad (4)$$

where λK label the multipolarity and magnetic component of the phonon operator. Each of these states represents the intrinsic component of the total wave function

$$\Psi_{nMK}^I = \sqrt{\frac{(1 + \delta_{K0})(2I + 1)}{16\pi^2}} \times [D_{MK}^I \Psi_{nK} + (-)^{I+K} D_{M-K}^I \Psi_{nK}], \quad (5)$$

where D_{MK}^I is the Wigner matrix. No free parameters are used in these calculations, and all physical input quantities and constants are determined by an independent fit to the experimental data in neighboring odd nuclei. For details see Ref. [41].

The experimental spectra of the 0^+ , 2^+ , and 4^+ states in ^{230}Th are compared with the results of the QPM calculations in Fig. 13. The QPM considers only vibrational 2^+ and 4^+ excitations in the even-even nuclei; therefore all other excitations have to be excluded from the comparison. Only the 2^+ and 4^+ states not belonging to rotational bands (see Sec. II C) are included in Fig. 13 (i.e., these states are assumed to be mainly of vibrational structure). The QPM generates 23 0^+ states below 2.8 MeV, in fair agreement with the 24 identified states. However, the QPM yields fewer 2^+ and 4^+ excited states than the ones observed experimentally. The numbers of 2^+ and 4^+ states generated up to 3 MeV are 20 and 17, respectively, considerably less than the observed 50 and 27 corresponding experimental levels (Fig. 13). It seems that taking into account the two-quasiparticle and pairing vibrational states not excluded from consideration (since there are problems in their identification) cannot explain this large difference. In addition to the ground state, experiment reveals one very strong peak for every 0^+ , 2^+ , and 4^+ state and small strengths for other states. The calculation correctly

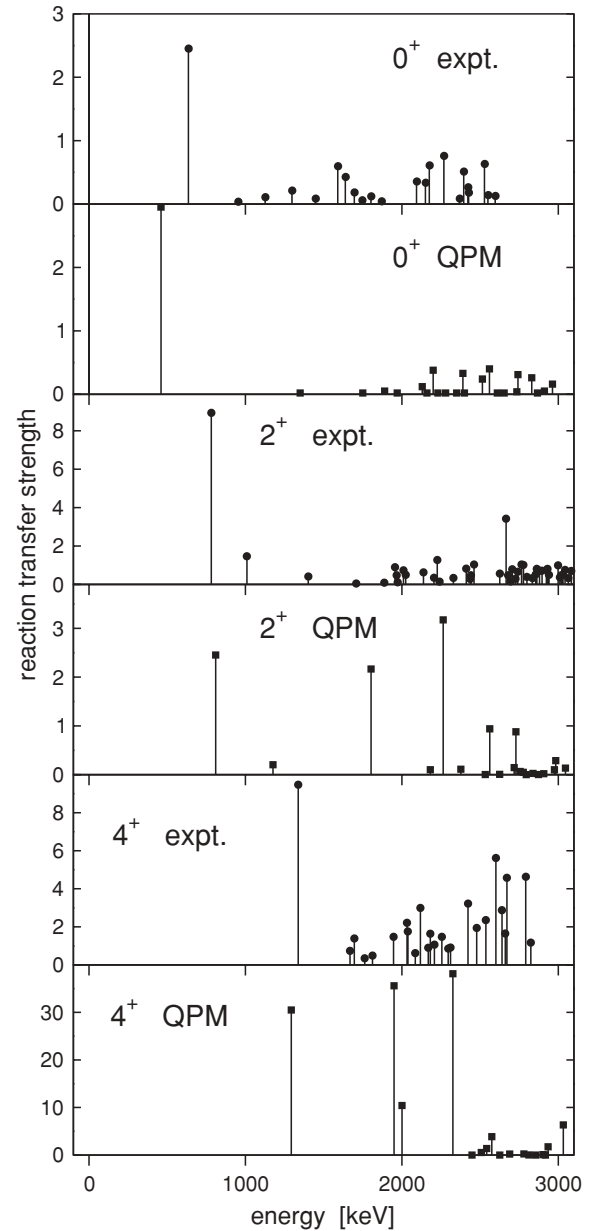


FIG. 13. Comparison of experimental and calculated (QPM) 0^+ , 2^+ , and 4^+ relative level reaction strengths for the (p,t) reaction. The 2^+ and 4^+ states assumed to belong to rotational bands (see Sec. II C) are not included. The experimental strengths for $0_{\text{g.s.}}^+$, 2_1^+ , and 4_1^+ being rotational states are normalized to 10 (but the latter two are not shown in figure).

yields strong peaks close in magnitude and position to the experimental ones for the 0^+ , 2^+ , and 4^+ states. These strong peaks form the suggested multiplet shown in Fig. 10. The calculation correctly yields small strengths for other peaks in the case of 0^+ excitations. Besides the first strong peaks, the QPM predicts for the 2^+ and 4^+ states two other strong peaks not observed experimentally.

In contrast to the *spdf*-IBM, the QPM is able to reproduce the two-neutron transfer strength. The wave functions [Eq. (5)] can be used to compute the (p,t) normalized transfer

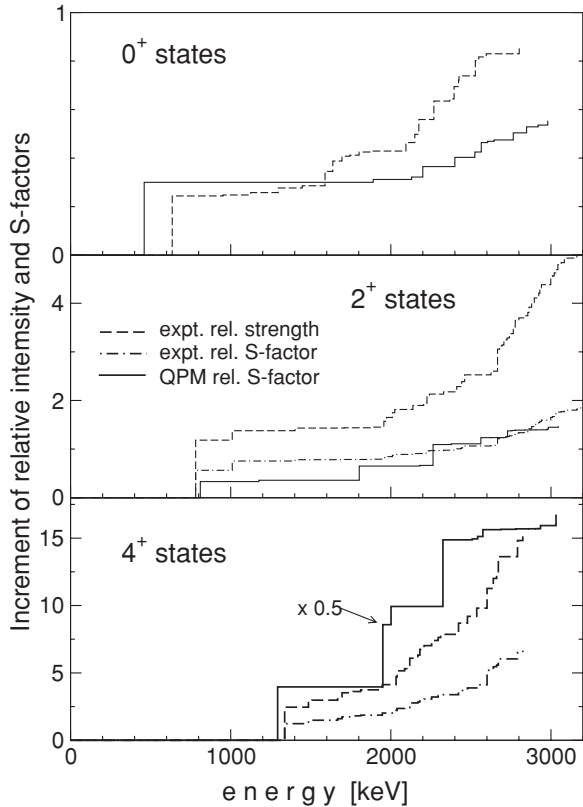


FIG. 14. Experimental increments of the (p,t) strength in comparison with the QPM calculations. The 2^+ and 4^+ states assumed as belonging to rotational bands (see Sec. II C) are not included.

spectroscopic factors

$$S_n(p,t) = \left[\frac{\Gamma_n(p,t)}{\Gamma_0(p,t)} \right]^2, \quad (6)$$

where the amplitudes are given by [48]

$$\Gamma_n(p,t) = \langle \Psi_{nMK}^I, N-2 | \sum_{q_1 q_2} r^I Y_{IK} a_{q_1} a_{q_2} | \Psi_0, N \rangle. \quad (7)$$

The amplitude $\Gamma_0(p,t)$ refers to the transitions to the I members of the ground-state rotational band [41]. In Fig. 14 we present the increments of the (p,t) strength to the 0^+ , 2^+ , and 4^+ states and that of the spectroscopic factors derived from the DWBA analysis for these states. They are given relative to those for corresponding states of the ground-state band and are compared with the calculated normalized spectroscopic factors. Since the DWBA analysis for the 0^+ states included different configurations of the transferred neutrons, only the (p,t) strength ratio is given in Fig. 14 for these states. For other states only the $(2g_{9/2})^2$ neutron configuration was accepted. According to the DWBA formalism in the case of the same neutron configuration and the direct one-step transfer the strength ratios have to be close to the spectroscopic factor ratios. This is not the case for ^{230}Th , since a considerable difference of these two ratios is observed.

As one can see, the calculations of 0^+ for the (p,t) strength ratio are in fair agreement with the experiment. For the 2^+ states the calculations are in good agreement with the measured

spectroscopic factor ratios; however, the measured strength ratios are nearly twice as large as calculated. We have to note that the (p,t) strengths for the 0^+ and 2^+ states not firmly assigned are small and do not influence considerably the results of comparison. Withdrawal of these states from consideration will only improve the agreement with the calculations. For the 4^+ states the calculated spectroscopic factors are more than twice the experimental strength and spectroscopic factor ratios. The difference possibly stems from the change of the (p,t) cross section caused by the inclusion of additional two-step paths of the neutron transfer for the 2^+ and 4^+ members of the ground-state band. As one can see from Fig. 7, the angular distributions for these states differ considerably from those for direct one-step transfer and can be fitted only by an inclusion of a two-step excitation number, which is the largest for the 4^+ state. For the 0^+ states, where only the one-step transfer is possible, the agreement between calculation and experiment is good. For both 2^+ and 4^+ states the energies at which the experimental strength first appears agrees with the calculated ones. This means that the energies of the first vibrational 2^+ and 4^+ excitations predicted by the QPM are in fair agreement with the experiment. (Recall that the states belonging to the rotational bands are excluded from this comparison.)

The nature of 0^+ excitations as well as of 2^+ and 4^+ states in the QPM differs greatly from that in the *spdf*-IBM. In all low-lying states quadrupole phonons are dominant and the octupole phonons are predicted to play a relatively modest role. This might be acceptable in the vibration-like ^{230}Th , but the same is predicted for the octupole-soft ^{228}Th . The spectrum is explained from the QPM calculation procedure (Pauli principle) as a redistribution of the strength of the lowest two-octupole phonons among many closely packed QPM 0^+ states [41]. To assess this aspect, calculations for octupole deformed lighter isotopes of Th would be important.

Other predictions of the QPM can be tested experimentally only for the lowest states. The measured values of $B(E2; 0_1^+ \rightarrow 2_0^+) = 1.1$ W.u. is close to the computed value of 1.7 W.u. However, the calculated monopole transition strength $\rho^2(E0; 0_1^+ \rightarrow 0_{g.s.}^+) = 1.48 \times 10^{-3}$ is two orders of magnitude smaller than the experimental value of $126(13) \times 10^{-3}$ [18]. Again, we would like to stress the necessity of systematic measurements of electromagnetic properties of higher excited 0^+ states to understand their nature.

IV. CONCLUSION

Excited states in ^{230}Th have been studied in (p,t) transfer reactions. About 200 levels were assigned by using a DWBA fit procedure. Among them, 24 excited 0^+ states have been found in this nucleus; most of them have not been experimentally observed previously. Their accumulated strength makes up more than 70% of the ground-state strength. Firm assignments have been made for most of the 2^+ and 4^+ states and for some of the 6^+ states. These assignments allowed the identification of sequences of states that have the features of rotational bands with definite inertial parameters. The 2^+ , 4^+ , and 6^+ states not included in these bands have been considered as vibration-like excitations. Multiplets of states are suggested that can be

treated as one- and two-phonon octupole quadruplets. The experimental data are compared with *spdf*-IBM and QPM calculations. Giving an approximately correct number of 0^+ states, these models provide different predictions for the structure of these states. They are also in conflict with the apparent structure of the states inferred from the moments of inertia of the rotational bands built on them. More specifically, as follows from the moments of inertia, the 0^+ states have a different intrinsic structures, which is in contradiction with the predictions of both the IBM (predominantly octupole bands) and the QPM (predominantly quadrupole bands). A remarkable feature of the QPM is the prediction of strong first vibrational excitations close in magnitude and position to the experimental ones. The numbers of 2^+ and 4^+ states are underestimated by both theories. Spectroscopic factors from the (p,t) reaction and the trend in their change with excitation energy are approximately reproduced by the QPM

for the 0^+ and 2^+ states and overestimated by theory for the 4^+ states. The lack of additional information does not allow for final conclusions on the validity of the theoretical approaches. Therefore we hope that our new data will stimulate further experimental and theoretical studies. Accurate experiments and a detailed analysis similar to that in the present work are desirable for other nuclei in this region. Challenging experiments on γ -ray spectroscopy following (p,t) reactions would give much needed information.

ACKNOWLEDGMENTS

We thank H. J. Maier for the preparation of the targets. The work was supported by the DFG (C4-Gr894/2-3, Gu179/3, and Jo391/2-3), MLL, and US Department of Energy Contract No. DE-FG02-91ER-40609.

-
- [1] P. A. Butler and W. Nazarewicz, *Rev. Mod. Phys.* **60**, 349 (1996).
 [2] J. V. Maher, J. R. Erskine, A. M. Friedman, R. H. Siemssen, and J. P. Schiffer, *Phys. Rev. C* **5**, 1380 (1972).
 [3] H.-F. Wirth, G. Graw, S. Christen, D. Cutoiu, Y. Eisermann, C. Günther, R. Hertenberger, J. Jolie, A. I. Levon, O. Möller, G. Thiamova, P. Thirof, D. Tonev, and N. V. Zamfir, *Phys. Rev. C* **69**, 044310 (2004).
 [4] A. I. Levon, J. de Boer, G. Graw, R. Hertenberger, D. Hofer, J. Kvasil, A. Löscher, E. Müller-Zanotti, M. Würkner, H. Baltzer, V. Grafen, and C. Günther, *Nucl. Phys.* **A576**, 267 (1994).
 [5] V. Yu. Ponomarev, M. Pignaneli, N. Blasi, A. Bontempi, J. A. Bordewijk, R. De Leo, G. Graw, M. N. Harakeh, D. Hofer, M. A. Hofstee, S. Micheletti, R. Perrino, and S. Y. van der Werf, *Nucl. Phys.* **A601**, 1 (1996).
 [6] A. M. Oros, P. von Brentano, R. V. Jolos, L. Trache, G. Graw, G. Cata-Danil, B. D. Valnion, A. Gollwitzer, and K. Heyde, *Nucl. Phys.* **A613**, 209 (1997).
 [7] Gh. Cata-Danil, D. Bucurescu, L. Trache, A. M. Oros, M. Jaskola, A. Gollwitzer, D. Hofer, S. Deylitz, B. D. Valnion, and G. Graw, *Phys. Rev. C* **54**, 2059 (1996).
 [8] D. A. Meyer, G. Graw, R. Hertenberger, H.-F. Wirth, R. F. Casten, P. von Brentano, D. Bucurescu, S. Heinze, J. I. Jerke, J. Jolie, R. Krücken, M. Mahgoub, P. Pejovic, O. Möller, D. Mücher, and C. Scholl, *J. Phys. G: Nucl. Part. Phys.* **31**, S1399 (2005).
 [9] D. Bucurescu, G. Graw, R. Hertenberger, H.-F. Wirth, N. Lo Iudice, A. V. Sushkov, N. Yu. Shirikova, Y. Sun, T. Faestermann, R. Krücken, M. Mahgoub, J. Jolie, P. von Brentano, N. Braun, S. Heinze, O. Möller, D. Mücher, C. Scholl, R. F. Casten, and D. A. Meyer, *Phys. Rev. C* **73**, 064309 (2006).
 [10] J. L. Egido and L. M. Robledo, *Nucl. Phys.* **A494**, 85 (1989).
 [11] A. I. Levon *et al.* (unpublished).
 [12] E. Zanotti, M. Bisenberger, R. Hertenberger, H. Kader, and G. Graw, *Nucl. Instrum. Methods A* **310**, 706 (1991).
 [13] H.-F. Wirth, Ph.D. thesis, Technische Universität München, 2001, <http://tumb1.biblio.tu-munchen.de/publ/diss/ph/2001/wirth.html>.
 [14] F. Riess, Beschleunigerlaboratorium München, Annual Report, 1991, p. 168.
 [15] G. Audi, A. H. Wapstra, and C. Thibault, *Nucl. Phys.* **A729**, 337 (2003).
 [16] Y. A. Akovali, *Nucl. Data Sheets* **69**, 155 (1993).
 [17] B. Ackermann, H. Baltzer, C. Ensel, K. Freitag, V. Grafen, C. Günther, P. Herzog, J. Manns, M. Marten-Tölle, U. Müller, J. Prinz, I. Romanski, R. Tölle, J. de Boer, N. Gollwitzer, and H. J. Maier, *Nucl. Phys.* **A559**, 61 (1993).
 [18] B. Ackermann, H. Baltzer, K. Freitag, C. Günther, P. Herzog, J. Manns, U. Müller, R. Paulsen, P. Sevenich, T. Weber, B. Will, J. de Boer, G. Graw, A. I. Levon, M. Loewe, A. Löscher, and E. Müller-Zanotti, *Z. Phys. A* **350**, 13 (1994).
 [19] P. D. Kunz, Computer code CHUCK3, University of Colorado (unpublished).
 [20] F. D. Becchetti and G. W. Greenlees, *Phys. Rev.* **182** 1190 (1969).
 [21] E. R. Flynn, D. D. Armstrong, J. G. Beery, and A. G. Blair, *Phys. Rev.* **182**, 1113 (1969).
 [22] F. D. Becchetti and G. W. Greenlees, in *Proceedings of the Third International Symposium on Polarization Phenomena in Nuclear Reactions, Madison, 1970*, edited by H. H. Barshall and W. Haeblerli (University of Wisconsin Press, Madison, 1971).
 [23] G. Ardisson, M. Hussonnois, J. F. LeDu, D. Trubert, and C. M. Lederer, *Phys. Rev. C* **49**, 2963 (1994).
 [24] I. Ragnarsson and R. A. Broglia, *Nucl. Phys.* **A263**, 315 (1976).
 [25] J. Gerl, Th. W. Elze, H. Ower, H. Bohn, T. Faestermann, N. Kaffrell, and N. Trautmann, *Phys. Rev. C* **29**, 1684 (1984).
 [26] R. Kulesa, Ch. Briancon, A. Lefebvre, C. F. Liang, J. P. Thibaud, R. J. Walen, A. Celler, Ch. Lauterbach, J. de Boer, Ch. Mittag, F. Riess, Ch. Schandera, H. Emling, S. Hlavac, R. S. Simon, I. N. Mikhailov, and Ph. N. Usmanov, *Z. Phys. A* **334**, 299 (1989).
 [27] D. R. Bess and R. A. Broglia, *Nucl. Phys.* **80**, 289 (1966).
 [28] R. A. Broglia, O. Hansen, and C. Riegel, in *Advances in Nuclear Physics*, edited by M. Beranger and E. Vogt (Plenum, New York, 1973) Vol. 6, p. 287.
 [29] D. R. Bess, R. A. Broglia, and B. Nilsson, *Phys. Lett.* **B40**, 338 (1972).
 [30] R. F. Casten, E. R. Flynn, J. D. Garret, O. Hansen, T. J. Mulligan, D. R. Bess, R. A. Broglia, and B. Nilsson, *Phys. Lett.* **B40**, 333 (1972).
 [31] R. F. Casten and P. von Brentano, *Phys. Rev. C* **50**, R1280 (1994).
 [32] H. Baltzer, K. Freitag, C. Günther, P. Herzog, J. Manns, U. Müller, R. Paulsen, P. Sevenich, T. Weber, and B. Will, *Z. Phys. A* **352**, 47 (1995).

- [33] H. Baltzer, J. de Boer, A. Gollwitzer, G. Graw, C. Günther, A. I. Levon, M. Loewe, H. J. Maier, J. Manns, U. Müller, B. D. Valnion, T. Weber, and M. Würkner, *Z. Phys. A* **356**, 13 (1996).
- [34] T. Otsuka and M. Sugita, *J. Phys. Soc. Jpn.* **58**, 530 (1989).
- [35] S. R. Leshner, A. Aprahamian, L. Trache, A. Oros-Peusquens, S. Deyliz, A. Gollwitzer, R. Hertenberger, B. D. Valnion, and G. Graw, *Phys. Rev. C* **66**, 051305(R) (2002).
- [36] N. V. Zamfir, J.-Y. Zhang, and R. F. Casten, *Phys. Rev. C* **66**, 057303 (2002).
- [37] Y. Sun, A. Aprahamian, J. Y. Zhang, and C. T. Lee, *Phys. Rev. C* **68**, 061301(R) (2003).
- [38] V. G. Soloviev, *Z. Phys. A* **334**, 143 (1989).
- [39] V. G. Soloviev, A. V. Sushkov, and N. Yu. Shirikova, *Nucl. Phys.* **A568**, 244 (1994); *Phys. Part. Nuclei* **27**, 667 (1996); *Prog. Part. Nucl. Phys.* **38**, 53 (1997).
- [40] N. Lo Iudice, A. V. Sushkov, and N. Yu. Shirikova, *Phys. Rev. C* **70**, 064316 (2004).
- [41] N. Lo Iudice, A. V. Sushkov, and N. Yu. Shirikova, *Phys. Rev. C* **72**, 034303 (2005).
- [42] W. I. van Rij and S. H. Kahana, *Phys. Rev. Lett.* **28**, 50 (1971).
- [43] A. V. Sushkov *et al.* (unpublished).
- [44] P. D. Cottle and N. V. Zamfir, *Phys. Rev. C* **58**, 1500 (1998).
- [45] P. D. Cottle and N. V. Zamfir, *Phys. Rev. C* **54**, 176 (1996).
- [46] N. V. Zamfir and D. Kusnezov, *Phys. Rev. C* **63**, 054306 (2001); **67**, 014305 (2003).
- [47] V. G. Soloviev, *Theory of Atomic Nuclei: Quasiparticles and Phonons* (Institute of Physics, Bristol, 1992).
- [48] R. A. Broglia, C. Riedel, and T. Udagava, *Nucl. Phys.* **A135**, 561 (1969).